U.PORTO
FEUP FACULDADE DE ENGENHARIA
UNIVERSIDADE DO PORTO

U.PORTO
INSTITUTO DE CIÊNCIAS BIOMÉDICAS ABEL SALAZAR
UNIVERSIDADE DO PORTO

Acute and developmental toxicity of gold nanorods on zebrafish (*Danio rerio*) embryos

Bárbara Sofia Maia Mesquita

Dissertation submitted in partial fulfillment of the requirements

For the Degree of Integrated Master in Bioengineering, Molecular Biotechnology

Supervisor: Dr. Sónia Fraga, PhD

Co-Supervisor: Dr. João Paulo Teixeira

Porto, September 2016

Acute and developmental toxicity of gold nanorods on zebrafish (*Danio rerio*) embryos

Bárbara Sofia Maia Mesquita

Submitted in partial fulfillment of the requirements

For the Degree of Integrated Master in Bioengineering, Molecular Biotechnology

Supervisor: Sónia Fraga, PhD (Postdoctoral Researcher, Department of Environmental Health, National Institute of Health Doutor Ricardo Jorge, Porto, Portugal and EPIUnit- Institute of Public Health, University of Porto, Porto, Portugal)

Co-Supervisor: João Paulo Teixeira, PhD (Assistant Researcher, Department of Environmental Health, National Institute of Health Doutor Ricardo Jorge, Porto, Portugal and EPIUnit- Institute of Public Health, University of Porto, Porto, Portugal)

Porto, September 2016

Some of the results included in this dissertation have been presented in scientific meetings:

Toxicity of gold nanorods on zebrafish (*Danio rerio*) embryos. Mesquita B, Fraga S, Simões AM, Lopes I, Teixeira JP. International Conference on Occupational & Environmental Toxicology, 21st-23rd June 2016, Porto, Portugal.

Toxicity of gold nanorods on zebrafish (*Danio rerio*) embryos. Mesquita B, Fraga S, Simões AM, Lopes I, Teixeira JP. XIV International Congress of Toxicology (IUTOX) 2nd-6th October 2016, Merida, Mexico.

Acknowledgments

I would like to start by thanking my research supervisor Dr. Sónia Fraga for the support, encouragement, friendship and for never letting me give up even when everything seemed to be falling apart. Undoubtedly, Dr. Sónia Fraga has contributed to my growth as a young scientist and her advices will follow me throughout my career.

I am also grateful to Dr. Isabel Lopes for the welcoming at the Biology Department of Aveiro University and the endless guidance and patience throughout the project. Additional thanks to Dr. João Paulo Teixeira for the opportunity that has given me to join his research team.

I could not forget to mention Dr. Isabel Sousa, Dr. Jorge Carneiro and Dr. Tiago Galvão from the CICECO-Centre for Research in Ceramics and Composite Materials, Aveiro University, for the valuable assistance on the characterization of the materials under evaluation. Additional thanks to Anabela Simões, Rita Almeida, Joana Santos and Abel Ferreira for teaching me all I should know about zebrafish and helping me throughout my experience in Aveiro University.

Thanks to all the staff of Environmental Health Department from National Institute of Health D. Ricardo Jorge (Porto) for the support and friendship. And an especial thank you to Dr. Susana Silva and Dr. Solange Costa, for their support, advice, encouragement and mostly for their friendship and kindness, which I will never forget.

I am also indebted to all my friends (Andreia Granja, Beatriz Queirós, Eva Carvalho, Lúcia Rebelo, Mariana Neves, Rita Pinto, Sílvia Fonseca, Sofia Assis and Sofia Moreira) that accompanied me in these 5 years and always pushed me to be the best I can possibly be.

At last, thanks to my family: my father, Alexandre; my mother, Alice and my sister, Filipa, who supported me throughout this whole academic journey, handled all my tears, my fears, my dramas and always believed in me. Mostly, thank you for doing everything you could to make sure nothing ever was missing. I would be nothing without you.

Abstract

Nanotechnology is one of the fastest growing areas and is expected to have a huge economic and social impact in the upcoming years. Gold nanomaterials (AuNMs), due to their unique optical-electronic properties, offer an opportunity for wide-ranging applications in diverse fields such as biomedicine, catalysis and electronics, and therefore are being focus of great attention. The large-volume manufacturing predicted for the next decades, with its subsequent release into the environment, coupled with the reactivity that arise at nanoscale have fostered the necessity to evaluate AuNMs risk for humans and ecosystems.

Accordingly, this study aimed to evaluate the acute and developmental toxicity of a commercial suspension of Au nanorods (AuNRs) capped with the cationic surfactant cetyltrimethylammonium bromide (CTAB), herein denominated as CTAB-AuNRs, to zebrafish (*Danio rerio*) early life stages. Zebrafish embryos were exposed to CTAB-AuNRs at concentrations ranging between 50 and 150 µg/L. Lethality and developmental endpoints such as hatching, edemas, malformations, heart rate, body length and development delays were assessed until 96 hours post fertilization (hpf). Sublethal concentrations were then used to investigate the internalization and the genotoxic potential of CTAB-AuNRs at 48 and 96 hpf zebrafish embryos. Uptake of the tested AuNRs was evaluated by quantifying the embryos Au content by Inductively Coupled Plasma-Optical Emission Spectrometry (ICP-OES), whereas DNA damage was assessed by the comet assay.

The CTAB-AuNRs induced 50% of mortality ($LC_{50,96hpf}$) at a concentration of 110.2 µg/L. In addition, at sublethal concentrations it was found to elicit development abnormalities such as tail deformities, pericardial edema, decreased body length and delays in the development of the eyes, head and tail elongation. Moreover, about 1% of the initial concentration of CTAB-AuNRs present in the exposure media was internalized by zebrafish embryos before (48 hpf) and after hatching (96 hpf). However, no DNA damage was induced by CTAB-AuNRs exposure. While mild malformations were observed, with a general all or nothing effect, the developmental delay observed coupled with the internalization of CTAB-AuNRs in zebrafish tissue might induce structural and functional changes that will only be unfolded later on with possible repercussions in the fitness of adult stages.

Overall, CTAB-AuNRs caused significant lethal and sublethal effects at low concentrations, highlighting the need to perform predictive risk assessment of these

nanomaterials in order to establish environmental safety values, support regulatory decisions and ultimately, assist the development of safer NMs and manufacturing processes.

Keywords: Nanotechnology, gold nanorods, ecotoxicity, genotoxicity, zebrafish embryos

Resumo

A nanotecnologia é uma das indústrias em maior crescimento e é expectável que tenha um grande impacto económico e social nos próximos anos. Os nanomateriais de ouro (AuNMs), devido às suas propriedades ótico-eletrónicas únicas, apresentam aplicabilidade em várias áreas como a biomedicina, catálise e eletrónica e, portanto, têm sido foco de grande atenção. A grande reatividade que surge à nano-escala aliada ao aumento do volume de produção de AuNMs e a sua subsequente libertação no meio ambiente, justifica a necessidade de avaliar o risco destes NMs para os humanos e o ecossistema.

Desta forma, este estudo teve como objetivo avaliar a toxicidade aguda e os efeitos nível do desenvolvimento embrionário de uma suspensão comercial de nano-bastonetes de Au revestidos com o surfactante catiónico brometo de acetiltrimetilamónio (CTAB), aqui designadas por CTAB-AuNRs, em embriões de peixe-zebra (*Danio rerio*). Estes foram expostos a concentrações entre 50 e 150 µg/L de CTAB-AuNRs e a letalidade e parâmetros de avaliação do desenvolvimento como a eclosão, edemas, malformações, batimento cardíaco, tamanho do corpo e atrasos no desenvolvimento, foram avaliados até às 96 horas pós-fertilização (hpf). Posteriormente, foram utilizadas concentrações subletais para investigar o potencial de internalização e genotoxicidade das CTAB-AuNRs em embriões às 48 e 96 hpf. A captação das AuNRs foi estimada através da quantificação de ouro nos embriões por Espectrometria de Emissão Atómica com Plasma Indutivamente Acoplado (ICP-OES) enquanto o dano no DNA foi aferido pelo ensaio do cometa.

A concentração letal média (CL_{50}) das CTAB-AuNRs às 96 hpf foi 110.2 µg/L. Ademais, concentrações subletais de CTAB-AuNRs induziram malformações como deformidades na cauda, edema no pericárdio, diminuição do tamanho e atrasos no desenvolvimento da cauda, olhos e cabeça dos peixe-zebra. Para além disso, cerca de 1% da concentração inicial de CTAB-AuNRs presente no meio de exposição foi detetada nos embriões tanto antes (48 hpf) como depois (96 hpf) da sua eclosão. Todavia, as CTAB-AuNRs não provocaram dano no DNA. Apesar das malformações observadas terem sido moderadas, os atrasos no desenvolvimento observados e a presença das CTAB-AuNRs no tecido dos peixes-zebra, poderá acarretar alterações estruturais e funcionais que apenas se irão manifestar mais tarde, com possíveis repercussões no fitness do peixe-zebra em adulto.

Resumindo, as suspensões de CTAB-AuNRs causaram letalidade e efeitos subletais significativos a concentrações baixas, o que realça a necessidade de realizar ensaios para prever o risco associado aos NMs de forma a estabelecer valores ambientais seguros, auxiliar na tomada de decisões regulamentares e por últimos, colaborar no desenvolvimento de NMs e processos de produção mais amigos de ambiente.

Palavras-chave: Nanotecnologia, nano-bastonetes de ouro, ecotoxicidade, genotoxicidade, embriões de peixe-zebra.

Table of Contents

List of Figures

List of Tables

List of Acronyms and Symbols

ADME	Absorption-Distribution-Metabolism-Elimination
Ag	Silver
Au	Gold
AuNMs	Gold nanomaterials
AuNRs	Gold nanorods
bw	Body weight
Cit	Citrate
CNS	Central Nervous System
CTAB	Cetyltrimethylammonium bromide
CTAB-AuNRs	AuNRs capped with CTAB
DLS	Dynamic Light Scattering
DMSO	Dimethyl sulfoxide
dpf	Days post-fertilization
EC	Environmental Concentration
EET	Extraembryonic tissues
EMEA	European Medicines Agency
FBS	Fetal bovine serum
FDA	Food and Drug Administration
FET	Fish Embryo Acute Toxicity Test
GSH	Glutathione
hESC	Human Embryonic Stem Cells
hpf	Hours post-fertilization
IM	Intramuscular
IV	Intravenous
LC_{50}	Median lethal concentration

LMP	Low melting point
LSPR	Localized Surface Plasmon Resonance
MEEE	2-(2-(2-mercaptoethoxy)ethoxy) ethanol
MES	Mercaptoethane sulfonic acid
NM	Nanomaterial
OECD	Organization for Economic Co-operation and Development
PBS	Phosphate-buffered saline
PEN	Project on Emerging Nanotechnologies
PTFE	Polytetrafluoroethylene
PVP	Polyvinylpyrrolidone
ROS	Reactive Oxygen Species
SEM	Standard error of the mean
TEM	Transmission Electron Microscopy
TG	Test guideline
TiO_2	Titanium dioxide
TMAT	Trimethylammonium ethanethiol
TPPMS	Mono-sulfonated triphenylphosphine
ZF	Zebrafish
Zn	Zinc
ZW	Zebrafish water

1. Introduction

1.1. Gold Nanomaterials (AuNMs): properties, applications and synthesis methods

Nanomaterials (NMs) are defined by the European Commission as “natural, incidental or manufactured materials containing particles, in an unbound state or as an aggregate or as an agglomerate and where, for 50 % or more of the particles in the number size distribution, one or more external dimensions is in the size range 1 nm - 100 nm” (in 2011/696/EU) (Commission 2011). Nanomaterials can be classified according to their chemical nature as carbon-based (e.g. fullerenes, carbon nanotubes, carbon black); metal-based (e.g. gold, silver, metal oxides, quantum dots) and organic-based (e.g. dendrimers and polymers). They can also be categorized according to their geometric configuration in spheres, shells, rods, wires, tubes, horns, thin films, coils and cones (Tiwari, Tiwari et al. 2012).

At nanoscale, the NMs exhibit a larger surface to volume ratio, which increases the number of active sites and surface area available to interact with diverse chemical species enhancing its chemical/catalytic reactivity, and its mechanic, optical, electrical and magnetic behavior (Oberdörster, Oberdörster et al. 2005). Due to these new or improved physicochemical properties compared to their bulk counterparts, engineered NMs hold great promise for an assortment of applications in a wide variety of fields, including biomedical, electronics, energy, environmental, and pharmaceutical industries. In fact, the global market for nanotechnology is expected to grow to $64.2 billion by 2019 as report by BCC Research (McWilliams 2014).

According to the Project on Emerging Nanotechnologies (PEN) online inventory, there are 1827 nano-enabled products already available on the market. Metal NMs,in particular silver (Ag) and titanium dioxide (TiO_2), are among the most used NMs found in consumer products (www.nanotechproject.org, last accessed September 13, 2016). The most recent update of PEN’s inventory of 2016 lists 442 and 92 Ag- and TiO_2NMs-based products, respectively. On the other hand, only 25 products containing gold nanomaterials (AuNMs) are listed in PEN, most of them in the cosmetic category (www.nanotechproject.org, last accessed September 13, 2016). However, AuNMs have been attracting great interest in the biomedical field as diagnostic and therapeutic tools due to their compatibility, and non-toxic and non-immunogenic nature (Howes, Rana et al. 2014) and in the electronics industry to enhance solar cells, liquid crystal displays and flash memory devices (Manheller 2012). Their global market size is likely to be worth 7 billion euros by 2020 (Global Markert Insights Insights 2016).

The AuNMs are characterized by localized surface plasmon resonance (LSPR), which occurs when an electromagnetic field drives the collective oscillations of a NM's free electrons into resonance, high molar extinction coefficients, broad energy bandwidth, excellent conductivity, catalytic activity, high surface area and stability (Saha, Agasti et al. 2012). These properties are easily tunable by varying particle size, shape, dispersity, and chemical environment. Shape anisotropy of gold nanorods (AuNRs) is a classic example of how geometry configuration remarkably influence the properties of NMs. Comparing to Au nanospheres, which possess a single LSPR peaks, AuNRs have two distinct plasmon resonances peaks owing to the two different axes (longitudinal and transverse) of the rods. Therefore, by varying the aspect ratio (length/diameter), the longitudinal LSPR can be tuned throughout the visible region of the spectrum and into the near-infrared region, which renders AuNRs with significantly different optical properties from Au nanospheres and long-term photostability (Burrows, Vartanian et al. 2016, Hinman, Stork et al. 2016).

Overall, these properties make AuNMs an exceptional component for bio-sensing and bio-imaging technologies (Saha, Agasti et al. 2012). Furthermore, as AuNMs can be easily functionalized with selective and specific recognition molecules (e.g. antibodies, natural ligands for certain receptors or peptides), they are being increasingly exploited as diagnostic tools to detect biomarkers of several diseases (Baptista, Doria et al. 2010, Zhou, Gao et al. 2015) and as drug delivery systems (Alkilany, Thompson et al. 2012, Kumar, Zhang et al. 2013). By loading the cargo on Au's surface through covalent or non-covalent binding and with proper functionalization, AuNMs can carry pharmaceutical drugs or other therapeutic molecules directly to the target site, which is of particular importance in cancer treatment as it enables the reduction of side effects and increases the therapeutic index. Recently, Amreddy, Narsireddy, et al. have successfully developed an AuNR-based drug delivery system, where the AuNRs were loaded with doxorubicin, a chemotherapeutic agent, conjugated with a pH-sensitive linker, and transferrin. Transferrin was used to target the overexpressed transferrin receptors in human lung cancer cells, whereas the pH-sensitive linker confines the release of doxorubicin to the acidic conditions of endosomes or lysosomes upon internalization of the AuNR by cancer cells (Amreddy, Muralidharan et al. 2015). Similar strategies such as PEGylation of AuNMs have also been applied to avoid phagocytic clearance by the reticuloendothelial system and immunogenic reactions, thus, enhancing circulation time (Ghosh, Han et al. 2008, Boccalon, Bidoggia et al. 2015). AuNMs are also suitable for hyperthermia in cancer treatment as they are able to convert absorbed light into heat

through a series of nonradiative processes (Huang and El-Sayed 2010, Khan, Vishakante et al. 2013).

A number of diagnostic devices comprising AuNMs have been already approved by the Food and Drug Administration (FDA) such as Verigene (Nanosphere) diagnostic tests to detect infectious pathogens and drug resistance markers, and First Response™ Pregnancy Tests from Church & Dwight Co., Inc. Although up to date no AuNM-base drug delivery system has been approved to clinical use, there are several of those currently under clinical trial. For instance, AurImmune™ (Cytimmune) has successfully attainned phase II clinical trial. This therapeutic platform, comprised by spherical AuNMs carrying tumor necrosis factor alfa (TNF-α), is design to penetrate the leaky blood vessels of tumors and specifically bind to TNF-α receptors on endothelial cells, acting as a Trojan Horse that enables follow-on chemotherapy to reach the tumor efficiently.

In the past few years, AuNMs have also been drawing attention to address environmental problems such as water pollution. AuNMs can be used as a platform to monitor the levels of toxic ions (e.g. arsenic, mercury, chromium), pesticides (e.g. atrazine, methylparathion) and pharmaceutical drugs (e.g. paracetamol, atenolol), and for aquatic environmental remediation (Saha, Agasti et al. 2012, Qian, Pretzer et al. 2013). Other potential applications of AuNMs include visual display technologies, such as touch sensitive screens, and advanced data storage technologies namely advanced flash memory devices.

Nanotechnology industry has been focused on the production of NMs with tailored size, shape, chemical composition and dispersity as NM's properties, and consequently their applications, are strongly dependent on these characteristics. Therefore, the optimization of synthesis methods has been object of intense research. The production of NMs, namely AuNMs, requires fine tuning of various parameters that influence the thermodynamic and kinetic aspects, and consequently determines the quality and yield of the synthesis (Scarabelli, Sánchez-Iglesias et al. 2015). Numerous strategies have been developed to synthesize AuNMs, the firstly reported was the reduction of Au salts in the presence of a reducing agent such as sodium citrate that initiates the nucleation of the Au ions, thus forming NMs. To prevent aggregation, a stabilizing agent is often added during synthesis (Turkevich, Stevenson et al. 1951, Frens 1973). To produce anisotropic AuNRs, the seed-mediated growth developed by Gearheart et al. is the most widely used method (Jana, Gearheart et al. 2001). In this technique, there is a temporal and spatial separation between the nucleation and

growth steps. Briefly, small spherical seeds are first produced from tetrachloroauric acid ($HAuCl_4$), an Au salt, and a strong reducing agent (e.g. sodium borohydride) that induces nucleation. Subsequently, these seeds are added to a growth solution that contains additional gold salt, a weak reducing agent (e.g. ascorbic acid) and a ‘‘soft template’’ [e.g. cetyltrimethylammonium bromide (CTAB)] that directs anisotropic growth. The ascorbic acid is commonly used to reduce the Au salt to elemental Au but this reaction only occurs in the presence of the seeds, otherwise it only reduces Au^{3+} to Au^{+} (Grzelczak, Pérez-Juste et al. 2008, Xia, Zhang et al. 2015). The CTAB, a cationic surfactant, guides the growth of Au seeds into rod-like shape by adsorbing preferentially to Au [100] and Au [110] crystal facets, over the Au [111] facets, which blocks the AuNM growth at the sides and induces the growth along the longitudinal axis as shown in **Figure 1** (Murphy, Thompson et al. 2011). Moreover, the positively charged bilayer of CTAB on AuNR’s surface creates mutual repulsions and prevents the aggregation of AuNRs, promoting their dispersity. However, CTAB is highly cytotoxic and for biomedical applications other strategies have been studied to replace this compound in the seed-mediated growth synthesis and still preserve the AuNRs properties (Gui and Cui 2012). Other production methods for anisotropic AuNMs include photochemical synthesis (Kim, Song et al. 2002) and electrochemical synthesis in solution (Yu, Chang et al. 1997) or in hard templates (Foss Jr, Hornyak et al. 1992).

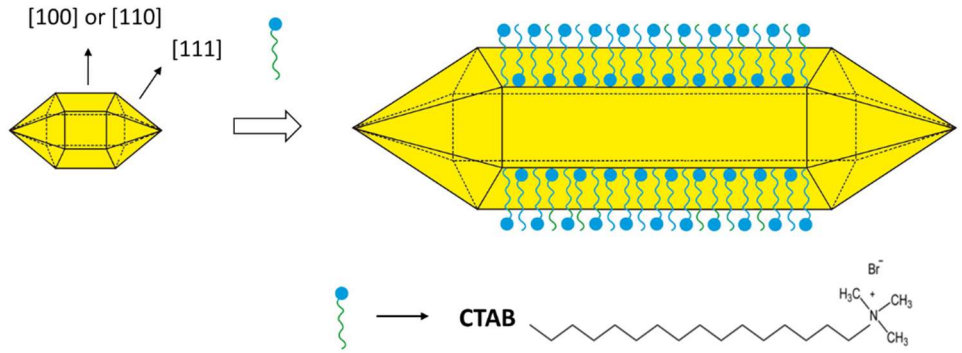

Figure 1 Scheme representing gold nanorods growth in the seed-mediated synthesis using CTAB that promotes anisotropic growth by adsorbing preferentially to Au [100] and Au [110] crystal facets, over the Au [111] facets [adapted from (Murphy, Thompson et al. 2011)].

1.2. Toxicology of AuNMs

Gold in the bulk form has for long been considered chemically inert, biocompatible, non-toxic and non-immunogenic (Howes et al., 2014). However, at nanoscale these metallic particles emerge as a catalyst with substantially different properties comparing to their bulk counterparts, which calls into question their safety.

Moreover, the increasing production and widespread application of AuNMs lead to their release into the different environmental compartments (e.g. soil, air and water), endangering human and environmental health.

As described in **Figure 2**, the release of NMs into the environment can occur at any stage of their life cycle, which begins with the processing of the raw materials and their transformation into NMs, followed by their incorporation into products, usage and ultimately disposal (e.g. landfills and waste incineration plants) (Sun, Gottschalk et al. 2014). The Ag- and TiO_2-NMs, for example, have been shown to be released from paints on building facades into urban runoff (Kaegi, Ulrich et al. 2008, Kaegi, Sinnet et al. 2010). Currently, there is no consistent data on environmental concentrations (EC) of NMs mainly due to the lack of appropriated separation and analytical methods. The few studies performed so far, mostly with Ag- and TiO_2-NMs, have used probabilistic material-flow modelling to predict the EC of NMs in surface water, waste water treatment plant, soils, sediments and atmosphere. For instance, gathering the data of the current literature on the topic, the modeled concentrations of TiO_2-NMs in surface water ranges from 3 to 1600 ng/L, whereas for Ag-NMs the predicted EC is slightly lower (between 0.1 and 1000 ng/L) (Gottschalk, Sun et al. 2013). In the case of AuNMs, Mahapatra et al. has reported that the estimated EC of AuNMs derived from nanomedicine products in surface water is approximately 0.468 and 0.0047 ng/L, respectively for the United Kingdom and United States of America (Mahapatra, Sun et al. 2015). On the other hand, according to Boxall et al., AuNMs derived from consumer products are present in water in concentrations ranging from 100 to 1430 ng/L (Boxall, Chaudhry et al. 2007). The high disparity of the predicted concentrations obtained in the different studies reflects the different estimations of NMs production and emission rates, as well as in NM product's market penetration. Moreover, the material flow analysis for NMs requires a fine understanding and description of the NM's flow chain, from resource extraction to final waste disposal. In addition, once introduced into the environment, NMs will establish diverse interactions with biotic and abiotic systems that will change their intrinsic characteristics and will further influence their fate and behavior in the ecosystem. These variables have not been taken into account in most of the material-flow analyses performed so far (Gottschalk, Sun et al. 2013) and thus further studies are required to fill in these gaps.

The employees of NM's companies, as shown in **Figure 2**, are the primary individuals at risk of exposure to NMs during manufacturing, packaging, handling, transport and disposal, followed by the consumers of nano-products. Therefore, it is important to define exactly what workers are exposed to in order to establish

occupational exposure limited values. Maynard et al., who inspected a single-walled carbon nanotube-generating operation, reported workplace air concentrations up to 53 $\mu g/m^3$ (Maynard, Baron et al. 2004). Furthermore, a study performed to assess the inhalation exposure of workers to metal oxides NMs associated with industrial wastewater treatment processes in a semiconductor research and development facility showed that NMs of 20.5 nm were present at concentrations greater than 100 particles/cm^3 during the execution of a specific task (Brenner, Neu-Baker et al. 2015). However, the available data regarding occupational exposure assessment of NMs is so far very limited, again due to the methodology required that is still under development. Up to date no study has been performed with AuNMs.

Taken together, it is essential to evaluate AuNMs risk for humans and ecosystems, understand their mechanism of action and the properties responsible by their toxicity in order to safeguard workers and consumers, establish environment safety values, support regulatory decisions and ultimately, assist the development of safer NMs and manufacturing processes.

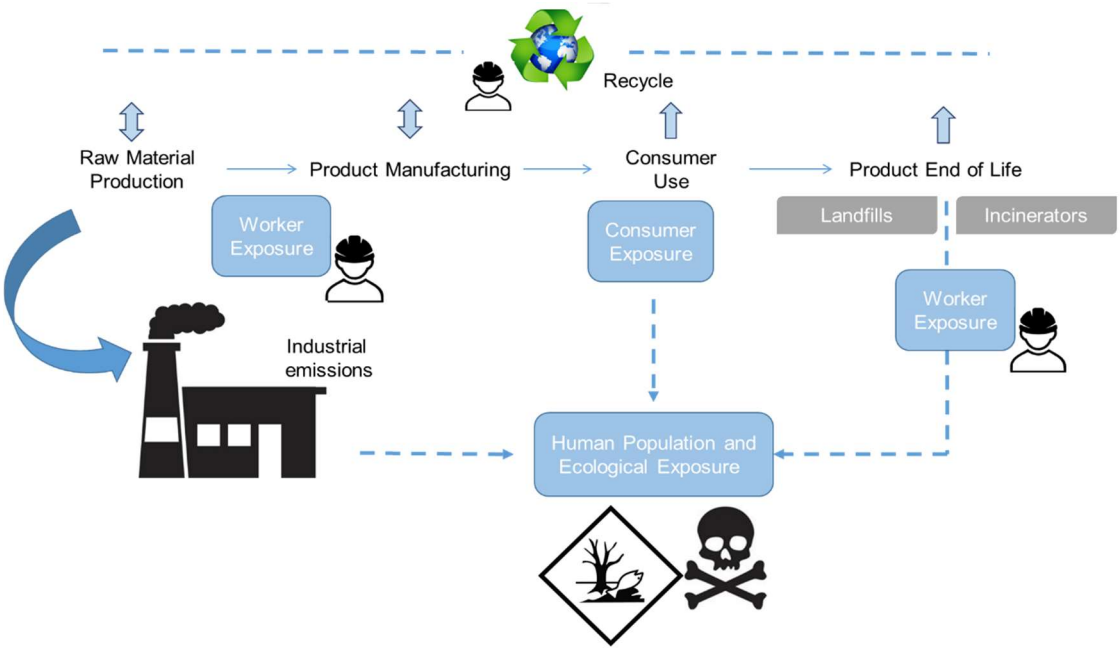

Figure 2 Nano-enable products life-cycle and possible stages for environmental and human exposure [adapted from (Initiative 2016)].

1.2.1. Human Exposure to AuNMs and the associated risks

Manufacturers and consumers of nano-enabled products are likely to be exposed to engineered NMs through different routes such as inhalation, dermal, oral, ocular, intravenous(IV) and intramuscular (IM), these latter two occurring almost exclusively in biomedical settings (Warheit and Sayes 2015). After exposure, the NMs

can translocate the biological barriers and reach the bloodstream, where they become coated with different proteins that adsorb to their surface, leading to the formation of a protein corona (Monopoli, Åberg et al. 2012). The nature of the corona formed is governed by the intrinsic characteristics of the NMs (e.g. chemical composition, surface chemistry, particle size, shape, charge and dispersion stability) (Mahmoudi, Lynch et al. 2011, Nel, Parak et al. 2015). These NM-protein complexes will subsequently dictate the tissue distribution of NMs and the interaction between NMs and cells. The biodistribution of AuNMs has also been reported to be dependent on their size, shape and surface chemistry (Janát-Amsbury, Ray et al. 2011, Morais, Soares et al. 2012, Han, Lee et al. 2015, Elci, Jiang et al. 2016). For instance, AuNMs of 13 and 105 nm were found to accumulate in lungs and translocate to bloodstream of Sprague–Dawley rats following inhalation of 12.8 ± 2.42 μg/m^3 for 5 days, however only the smaller ones were detected in the liver, spleen, brain and testes (Han, Lee et al. 2015). Furthermore, AuNMs have been shown to accumulate preferentially in the liver and spleen following intravenous injection, which might result from the capacity of the reticuloendothelial system to remove particulate matter from circulation (Semmler-Behnke, Kreyling et al. 2008, Cho, Cho et al. 2009).

AuNMs have generally been considered biocompatible, however the potential biopersistence of AuNMs in the organism allied to their catalytic activity might result in long-term chronic effects. In some studies, these NMs have been reported to cause fatigue, decreased appetite, weight loss (Chen, Hung et al. 2009, Zhang, Wu et al. 2010), altered gene expression pattern (Balasubramanian, Jittiwat et al. 2010), spleen atrophy and mild anemia (Fraga, Brandao et al. 2014) in exposed rodent models. Nevertheless, it has been pointed out that the main reason for some of the toxic effects detected might be the adsorbed molecules on the AuNM's surface, used to increase NMs dispersion and stability in aqueous media, or impurities derived from the synthesis process, rather than to the AuNMs *per se* (Alkilany and Murphy 2010). Therefore, the toxicity of pristine, surface-modified and functionalized NMs should be carefully distinguished.

1.2.2. **Ecotoxicology of AuNMs in aquatic environments**

In the aquatic environment, the NMs can be suspended in the water phase or deposited in the sediment, depending on their primary characteristic and their interaction with abiotic systems. For instance, factors such as salinity, temperature, pH and natural organic matter content will determine agglomeration and aggregation status, dissolution, redox reactions, surface transformation and sedimentation of NMs

and therefore their bioavailability for the aquatic species (Wang, Zhang et al. 2016). The NMs associated with the sediment will interact directly with benthic species, whereas NMs suspended in the water column will be bioavailable for algae, invertebrates and fish (Amiard-Triquet, Amiard et al. 2015). Moreover, organisms can interact directly with NMs through adsorption and subsequent internalization, or may be taken up via trophic transfer. Recently, it was demonstrated that AuNRs are able to pass from the water column to the marine food-web (Ferry, Craig et al. 2009). Moreover, AuNMs have been detected in *Daphnia magna* fed with the unicellular microorganisms *Chlamydomonas reinhardtii* and *Euglena gracilis* previously exposed to these nanoparticles (Lee, Yoon et al. 2015). These studies indicate that AuNMs are indeed able to accumulate at the lowest trophic levels (e.g. microorganisms and invertebrates) and to be transferred to the highest trophic levels (fish and possibly humans) through the food chain.

Up to date, few studies on the biodistribution and toxicity of AuNMs in aquatic organisms have been undertaken. Nevertheless, the current literature indicates that AuNMs are able to accumulate and induce toxicity at some extent in different levels of the trophic cascade. The AuNMs have been shown to accumulate in the digestive tract of both aquatic invertebrates and fish following exposure to concentrations ranging from 0.5 to 100 mg/L, and 20 mg/L, respectively, although no hazard has been reported (García-Cambero, García et al. 2013, Botha, Boodhia et al. 2016). On the other hand, juvenile marine fishes (*Pomatoschistus microps*) exposed to 0.2 mg/L of AuNMs were shown to have decreased predatory performance, which in the wild might reduce the individual fitness, compromising population growth and survival (Ferreira, Fonte et al. 2016). The exposure of marine bivalve *Scrobicularia plana* to 100 µg/L of differently sized (5, 15 and 40 nm) AuNMs has shown to negatively impact the burrowing speed and to increase the levels of the enzymes involved in the antioxidant defense mechanisms, although the feeding behavior was not affected (Pan, Buffet et al. 2012). Furthermore, 40 nm AuNMs coated with polyvinylpyrrolidone (PVP) at 4, 80 and 1600 µg/ L were reported to increase the hepatic expression of antioxidant, immune and apoptosis related-genes mRNA levels in exposed *Sparus aurata* fishes (Teles, Fierro-Castro et al. 2016).

1.2.3. **Mechanism of AuNMs toxicity: focus on genotoxicity**

Oxidative stress, inflammation and genotoxicity seem to be the three main mechanisms underlying NMs toxicity (Fadeel and Pietroiusti 2012). Oxidative stress is caused by an excessive reactive oxygen species (ROS) production and/or a decrease

in the antioxidant defenses, which can damage cells through lipid peroxidation, DNA/protein oxidation or by interfering with signaling pathways and gene function. Additionally, oxidative stress may initiate an inflammatory signaling cascade and ultimately induce cell death. Cytotoxicity of metallic NPs have been extensively explored in *in vitro* and *in vivo* studies and can be reviewed elsewhere (Lewinski, Colvin et al. 2008, Arora, Rajwade et al. 2012).

Genotoxicity induced by NMs, which encompasses all types of DNA or chromosome damage (e.g. strand breaks, adducts rearrangements, mutations, chromosome aberrations and aneuploidy), is less explored and data obtained are frequently controversial. Nevertheless, it appears that genotoxic effects induced by metal NMs can arise either through direct interaction of the NMs with the genetic material or indirectly by elevation of ROS levels (Dusinska, Magdolenova et al. 2013). By interacting directly with DNA, NMs can produce a variety of DNA lesions including simple base modifications, base mismatches, double-strand breaks and bulky DNA adducts. These lesions can give rise to further gene mutations and chromosomal damage (numerical or structural) if not repaired (Golbamaki, Rasulev et al. 2015). Aneugenic events may also be caused during cell division by interaction of NMs with the mitotic spindle apparatus, centrioles or their associated proteins (Huang, Chueh et al. 2009). Di Bucchianico et al. conducted a study to investigate the ability of 5 and 15 nm AuNMs to induce genotoxic events in human primary lymphocytes and murine macrophages and observed a significant increase in both primary and oxidative DNA damage after 2 and 24 h of exposure to different concentrations (0.1, 1, 10, and 100 μg/mL) of these NMs. In addition, a concentration dependent increase in the frequency of micronuclei (MN) was observed in both cell types. In order to distinguish between MN originated from chromosome fragments or whole chromosomes that lag behind at anaphase during nuclear division, the authors used Fluorescent In Situ Hybridization (FISH)-pancentromeric probes. Data showed that MNs were centromere-positive, which indicate that aneugenic rather than clastogenic events were induced by tha AuNMs (Di Bucchianico, Fabbrizi et al. 2014).

Interaction with DNA-related proteins, namely the ones involved in the replication process, transcription and damage repair, has also been shown to play a role in the genotoxic potential of metal oxide NMs (Magdolenova, Collins et al. 2014, Golbamaki, Rasulev et al. 2015). Indeed, DNA damage as well as altered expression of proteins associated with cell cycle regulation and DNA repair were observed in MRC-5 human fetal lung fibroblast cells exposed to AuNMs (Li, Lo et al. 2011).

NMs have also been shown to induce DNA damage through secondary mechanisms such as oxidative stress. Indeed, ROS generation has been considered the main mechanism of DNA damage resulting from exposure to NMs. Excessive ROS levels can cause the depletion of the antioxidant defenses together with oxidative modifications in the DNA, including strand breaks and base oxidation [e.g. 8-hydroxy-2′-deoxyguanosine (8-OHdG)] (Wan, Mo et al. 2012, Magdolenova, Collins et al. 2014). Moreover, DNA damage *in vivo* can also be induced as a secondary response to inflammation triggered by NMs (Downs, Crosby et al. 2012).

Following DNA damage cells activate complex signaling networks which promote either DNA repair/survival or cell death (Roos, Thomas et al. 2015). The final outcome, i.e. survival or death, is dependent on several factors, namely cell tolerance to damage and/or magnitude of the impairment in DNA repair mechanisms caused by the NMs, which as mentioned above may have an important part in genotoxic events (Magdolenova, Collins et al. 2014).

Although there are only few *in vivo* studies focused on the genotoxicity of AuNMs, the results in general are negative for both DNA damage and clastogenic/aneugenic potential. Downs et al. showed accumulation of AuNMs of different sizes (2, 20, 200 nm) in the liver and lung tissues of rats exposed through IV injection to 0.030 mg/kg body weight (bw). However, this tissue accumulation was neither translated into an increase in DNA damage in liver, lung and white blood cells nor into an increase in the % of MN in circulating reticulocytes (Downs, Crosby et al. 2012). In another study, neither DNA damage in lung cells nor augmented frequency of MN in polychromatic erythrocytes was identified 3 days after single intratracheal instillation of 36 µg/mL AuNMs of different sizes (2, 20 or 200 nm) in male rats (Schulz, Ma-Hock et al. 2012). In contrast, oral exposure to AuNMs for 7 or 14 days increased the frequency of MN in polychromatic erythrocytes at 320 mg/kg bw and the formation of DNA adducts in hepatic cells at 160 and 320 mg/kg bw. These findings suggests that AuNMs exposure can induce oxidative stress-mediated genomic instability (Girgis, Khalil et al. 2012). Nevertheless, adequate *in vivo* studies using doses and exposure periods that represent realistic scenarios are still lacking.

Considering the potential application of AuNMs in the medical field, the surface modification of NMs can be a good strategy to protect cells from the undesirable genotoxic effects of AuNMs. Bearing that in mind, Fraga et al. studied the genotoxicity of AuNMs coated with citrate (Cit) or 11-mercaptoundecanoic acid (11-MUA) in human liver HepG2 cells. Both differently coated AuNMs were taken up by HepG2 cells,

however only Cit-AuNMs induced significant DNA damage. Interestingly, the genotoxicity observed was inversely proportional to the tested concentrations (0.1, 1 and 10 µM) (Fraga, Faria et al. 2013). On the other hand, Hashimoto et al. did not find any significant DNA damage either in L929 fibroblast or Raw macrophage cells exposed to 100 and 400 µg/mL of citrate-coated AuNMs (Hashimoto, Kawai et al. 2016). In addition, sophorolipid reduced AuNMs, which have been explored as drug delivery systems, have not induced DNA breaks at 0.5, 5 and 50 µg/mL in HepG2 cells (Singh, D'Britto et al. 2010).

1.3. Zebrafish (*Danio rerio*) as an alternative animal model to assess toxicity

Zebrafish (*Danio rerio*) is a small tropical fish, originally found in the rivers of India and South Asia, that has become one of the most popular model organism for (eco)toxicology, vertebrate development and human disease studies. Zebrafish offers several technical advantages over other animals used in experimental research, such as rapid development, high fecundity, generation of transparent embryos that develop outside the mother's body (allowing the *in vivo* visualization of cell-biological events), low maintenance costs and ease of manipulation (Scholz, Fischer et al. 2008). Furthermore, the genomic sequencing of zebrafish is highly advanced and various DNA libraries, microarray resources, and protocols for generating transgenic fish and knocking down gene expression in embryos have been developed and widely established (Stegeman, Goldstone et al. 2010).

The adult zebrafish is used as a model in environmental toxicology for hazard identification and risk assessment of chemicals, plant protection products, pharmaceuticals, biocides, feed additives, and effluents. In 2013, the fish embryo acute toxicity test (FET) with zebrafish embryos was approved by the Working Group of the National Coordinators of the OECD Test Guideline Program and published as OECD test guideline (TG) no. 236. This test guideline is intended to determine the acute or lethal toxicity of chemicals in early-life stages of zebrafish, but can also be used as an alternative to the fish acute test [OECD TG 203; (OECD 1992)] as zebrafish embryos were shown to have similar toxicological profiles for hazardous agents with various adult fish species commonly tested (Braunbeck, Kais et al. 2015).

Zebrafish has a high degree of genetic, molecular and physiological similarity with mammals and has been shown to exhibit very similar Absorption-Distribution-Metabolism-Elimination (ADME) profiles to rodent models and humans, which explains their increasing use as a model for drug discovery and to predict the toxic potential of

different compounds (Yang, Ho et al. 2009, Bailey, Oliveri et al. 2013, MacRae and Peterson 2015). In that respect, the FDA and European Agency for the Evaluation of Medicinal Products (EMEA) have recently accepted zebrafish's pharmacology and toxicology data for preclinical trials to evaluate whether a new drug is safe or not for human testing, a requirement to obtain regulatory approval for a clinical trial (He, Gao et al. 2014). One example of a disease-relevant compound that has been tested in zebrafish is ProHema, a stabilized derivative of prostaglandin E2, which was found to increase the numbers of hematopoietic stem cells (North, Goessling et al. 2007). This compound is currently under Phase II trials in patients undergoing umbilical cord blood transplantation for leukemia or lymphoma as it might improve the effectiveness of transplantation by enhancing the rate of bone marrow recovery (MacRae and Peterson 2015).

1.3.1. **Stages of embryonic development**

The embryonic development of zebrafish starts when the eggs, spawned by females, are fertilized by sperm released by males into the water. After fertilization, the zygote undergoes a series of cleavage stages at the animal pole, which results in a flattened blastodisc at the periphery. The following period named gastrula is characterized by the transformation of the blastodisc to ball-like shape and the beginning of the epiboly, where the blastodisc spreads over the yolk in the vegetal pole direction. In the gastrulation stage, which occurs between 5-10 hours post fertilization (hpf), the embryo is converted into a structure of three germ layers - ectoderm, endoderm and mesoderm. These germ layers will give rise to all tissues in the organism. At 10 hpf, the gastrulation and epiboly are completed and the embryo has an anteroposterior axis with the contours of head and tail. During the segmentation period (10-24 hpf) takes place the development of somites, which are blocks of segmental mesoderm that establish the segmental organization of the body. Moreover, rudimentary organs, such the eyes and the brain, become evident and the embryo elongates with the detachment of the tail as illustrated in **Figure 3 (1).** The heartbeat of zebrafish embryo begins at 22 hpf, followed by the blood flow at 24 hpf. Between 24 and 48 hpf, pigmentation becomes observable in the eyes and body and the skeletal muscle starts to contract spontaneously [**Figure 3 (2)]**. At the end of 48 hpf, the organogenesis is almost complete and the embryo is motile and responsive to external stimuli. The embryos hatch from the chorion approximately between 48 and 96 hpf, and eleutheroembryo stage ensues but the embryo is still dependent on the yolk for food supply [**Figure 3 (3)]**. At 96 hpf occurs the formation of the pectoral fins [**Figure 3 (4)]** and the inflation of swim bladder [**Figure 3 (5)]**, essential for fish to achieve neutral

buoyancy with minimal energy expenditure (Kimmel, Ballard et al. 1995, Rosenthal and Harvey 2010). At 5 days post fertilization (dpf), the zebrafish embryos fully depleted the yolk and start the external feeding, therefore reaching the larvae stage. The adult period begins with the sexual maturation, which can be attained at the age of 3 months (Scholz, Fischer et al. 2008).

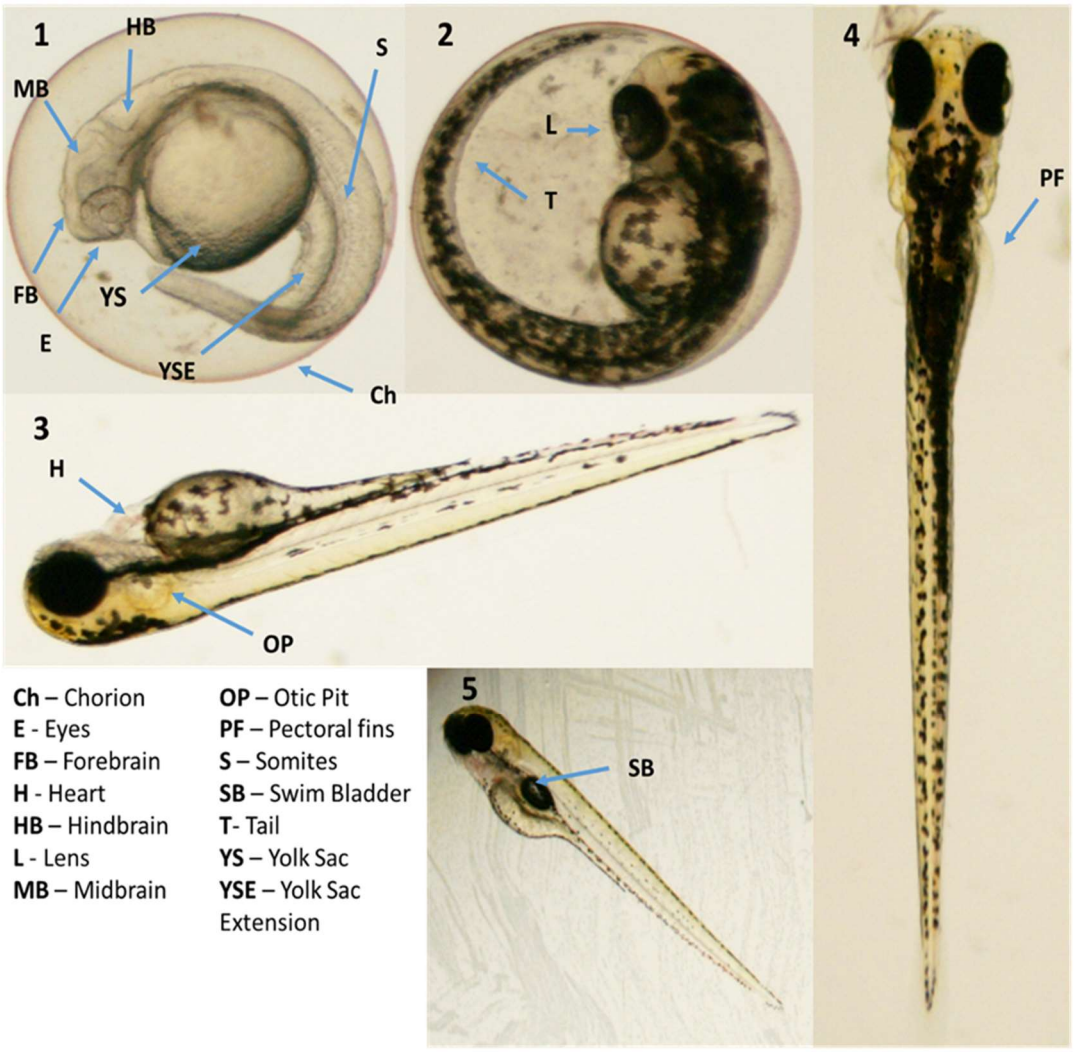

Figure 3 Development stages and main structural features of zebrafish. Zebrafish embryos at 24 hpf (1), 48 hpf (2), 72 hpf (3) and 96 hpf (4 and 5) (Kimmel, Ballard et al. 1995).

1.4. Toxicity of AuNMs towards more susceptible life stages

As the likelihood of organisms being exposed to NMs increases, there are raising concerns regarding their potential to cause reproductive toxicity, which includes adverse effects on sexual function and fertility in adult males and females, as well as developmental toxicity in the progeny. Developmental toxicity might manifest as death,

structural abnormalities (malformations), growth retardation, behavioral and functional abnormalities. These effects can result from exposure of either parent prior to conception or during prenatal development (OCDE 2008). The embryonic period, more specifically during pre-differentiation, early-organogenesis and late-organogenesis, is when the developing organs are most vulnerable to toxic substances as embryonic cells have immature repair and detoxification mechanisms, and the development process requires precise temporal-spatial sequencing (Hansen and Harris 2013, Dutta 2015). Moreover, in the case of mammals, placenta *per se* does not guaranty safety for the fetus, as it is permeable to many substances. In fact, it has been shown both *in vivo*, in animal models, and *ex vivo*, in the human placental perfusion model, that NMs may indeed pass through the placenta (Myllynen, Loughran et al. 2008, Chu, Wu et al. 2010, Grafmüller, Manser et al. 2013). Therefore, exposure to NMs might interfere with the normal developmental course of the embryo and cause permanent defects. In the case of aquatic organisms, the exposure of early-life stages to these xenobiotics can further result in reduced fitness, susceptibility to predation in the wild, lower reproductive rates, or to the development of carcinogenesis, endocrine, and immune system defects (Embry, Belanger et al. 2010).

Interestingly, so far no effects were detected on mammalian embryos after AuNMs exposure. According to Yang et al., there is a higher accumulation of AuNMs in the fetus at early pregnancy stages (below gestational day 9.5) than at gestational day 11.5 or above, while the accumulation in the extraembryonic tissues (EET) increases with the gestational age. The time frame at which these change occurs coincide with the maturation of placenta that seems to decrease the fetal exposure to NPs (Yang, Sun et al. 2012). Moreover, it has been shown a higher accumulation in fetus and EET of ferritin and polyethylene glycol (PEG)-coated AuNMs than of citrate-capped NPs. The latter coating has a negative charge, which might explain its reduced accumulation (Yang, Sun et al. 2012). Furthermore, Semmler-Behnke et al. reported that after a single IV administration of three differently sized AuNMs (14, 18 and 80 nm at 5.2, 3.2 and 26.5 µg/rat, respectively) at gestational day 18, all three AuNMs were detected in the EET, while only 14 and 18 nm AuNMs were observed in the fetus. These results seem to indicate that the AuNMs accumulation in the fetus is size-dependent. In that matter, the authors suggested that AuNMs translocation across the placental tissues occurs through transtrophoblastic channels and/or via transcellular processes, which further indicates the important role of placenta in embryo toxicity (Semmler-Behnke, Lipka et al. 2014). Altogether, these results showed that the gestational age at which pregnant mice are exposed, NM size and surface composition greatly impact AuNMs

distribution in fetus and EET. Considering these results it would be expected that the extent of impairment of fetal and postnatal development would be higher at early gestational exposure as it results in higher accumulation in the fetus. However, it has been shown that prenatal exposure to AuNMs did not affect the offspring independently of the gestational age (Yang, Sun et al. 2012). Furthermore, an *in vitro* study revealed that injection of 50 μg/mL of AuNMs into 2-cell mice embryo have not interfered with blastocyst rate or the expression of genes involved in embryo development (Taylor, Garrels et al. 2014). Nevertheless, it should be highlighted that this study lack of the evaluation of important parameters to determine embryo quality for implantation success such as cleavage rate, cell number, symmetry and shape of the blastomeres and cytoplasmic fragmentation extent in the perivitelline space.

In regard to the potential toxicity of AuNMs towards early-life stages of fish, AuNMs have been reported to diffuse through the chorionic pore canals and reach the inner cell mass of zebrafish embryos, remaining inside them throughout the entire development (Browning, Lee et al. 2009, Browning, Huang et al. 2013). Furthermore, Browning et al. reported that the effects of AuNMs in the zebrafish embryo development are minimal and dependent of NM size with smaller NMs (11.6±0.9 nm) inducing higher mortality and deformities than larger AuNMs (86.2±10.8 nm) at the same administered doses (Browning, Lee et al. 2009, Browning, Huang et al. 2013). Other studies reported no obvious abnormalities in the zebrafish embryos development after exposure to bare or polyvinyl alcohol (PVA)-capped AuNMs (Asharani, Lianwu et al. 2011, Kim, Zaikova et al. 2013). On the other hand, Truong et al. investigated the influence of functional groups on the toxicity induced by AuNMs. AuNMs functionalized with the positively charged trimethylammonium ethanethiol (TMAT) were shown to induce embryo lethality, while AuNMs functionalized with the negatively charged mercaptoethane sulfonic acid (MES) caused sub-lethal malformations to the embryos (Truong, Tilton et al. 2013). Moreover, both types of NMs were shown to cause misregulation of genes associated with immune response, and inflammation processes and behavioral abnormalities that were extended to the adulthood (Truong, Saili et al. 2012, Truong, Tilton et al. 2013). On the contrary, AuNPs functionalized with the neutral 2-(2-(2-mercaptoethoxy)ethoxy) ethanol (MEEE) did not induce toxicity (Truong, Tilton et al. 2013). Furthermore, TMAT ligands were also shown to affect eye development through an increase in the apoptotic process and downregulation of genes involved in eye formation, and to impair swimming behavior and axonal growth (Kim, Zaikova et al. 2013). Mono-sulfonated triphenylphosphine (TPPMS) and glutathione (GSH) ligands are being explored for AuNMs stabilization and for

therapeutic purposes (Leifert, Pan-Bartnek et al. 2013). Yu Pan et al. evaluated the teratogenicity of these coatings in zebrafish embryos and verified that AuNMs carrying TPPMS where much more toxicity than AuNMs carrying GSH. These authors observed that TPPMS-AuNMs caused 100% lethality at 400 μM and peripheral edema, cardiac malformations and hypopigmentation at sub-lethal doses. In addition, co-incubation of TPPMS-AuNMs with GSH, a ROS scavenger, decreased significantly the malformations, which suggests that toxicity of TPPMS-AuNMs was due to oxidative stress (Pan, Leifert et al. 2013). These studies demonstrated that AuNMs functionalization and particularly the charge, either positive or negative, have a significant impact on zebrafish development. Ionic concentration of the exposure medium was also shown to influence AuNMs toxicity. As ionic concentration decreases, the dispersity of AuNMs increases, which causes an increase in mortality, malformation and behavioral deficits of zebrafish embryos (Truong, Zaikova et al. 2012).

Although up to date it has not been reported noteworthy teratogenic effects of AuNMs *in vivo*, a few studies have shown that these NMs might interfere with Central Nervous System (CNS) development. The AuNMs were found to be highly toxic for human embryonic stem cells (hESC), whose differentiation into neurons mimics early stages of human brain development, in a size-dependent manner. The AuNMs of 1.5 nm adversely affected hESC survival and neuronal differentiation at 0.6 or 10 μg/mL, whereas 4 or 14 nm AuNMs did not induce toxicity. Exposure to 1.5 nm AuNP have also resulted in cell death of hESC-derived neural progenitor cells (Senut, Zhang et al. 2015). Furthermore, Söderstjerna et al. reported that AuNMs of 20 and 80 nm significantly affected the sphere size and morphology of human embryonic neural precursor cells (Söderstjerna, Johansson et al. 2013). Consequently, further studies are needed to confirm the real extent of AuNMs toxicity in embryo development as although no obvious malformations were observed, its accumulation may induce more subtle alterations particularly at cellular level.

2. Scope and Aims

Nanotechnology is expected to have a huge economic and societal impact worldwide within the next few years. Due to their unique optical-electronic properties, AuNMs have received great attention and therefore are being increasingly investigated and used in various commercial, industrial and biomedical applications. The high reactivity that may arise at nanoscale and the comparable dimensions between cellular components and NMs might lead to harmful interactions between them, which have brought into question NMs safety. Owing to the inert and biocompatible nature of Au in the bulk form, AuNMs were initially regarded as nontoxic and less scrutinized in terms of their safety evaluation and risk assessment. Nevertheless, considering the socioeconomic impact that AuNMs are expected to reach in the upcoming years and their release into the environment, it is crucial to determine the implications of exposure to these NMs, particularly the ones already available in the market, on both organisms and the ecosystems. Indeed, NMs may enter the aquatic system, accumulate in sediments and result in multi-component mixtures posing different threats not only to wildlife but also to humans.

In this context, the main goal of this study was to evaluate the acute and developmental toxicity of a commercial suspension of Au nanorods (AuNRs) capped with the cationic surfactant cetyltrimethylammonium bromide (CTAB), herein designated as CTAB-AuNRs, to early life stages of biota, which are the most sensitive life cycle stage and often highly predictive of xenobiotics toxicity in the adult stage. Zebrafish (*Danio rerio*) embryos were chosen since they are recognized as a suitable and relevant model for (eco)toxicological studies, with a high degree of genetic, molecular and physiological similarity to humans and a good alternative to animal testing following the 3R'S principle. Therefore, zebrafish embryos allow the analysis of multiple endpoints ranging from acute to developmental toxicity determination.

To achieve this main objective, four specific goals were established:

i. To characterize the colloidal suspensions in terms of particle size, size distribution, morphology and zeta potential as the toxicological potential of the NMs is highly dependent on their physicochemical characteristics;
ii. To assess the lethality, acute toxicity and developmental effects, including embryo development delays and malformations, of CTAB-AuNRs to zebrafish embryos;
iii. To confirm whether or not CTAB-AuNRs are internalized by the exposed zebrafish by assessing the embryo Au content at different time-points (before and shortly after hatching);

iv. To investigate the genotoxic potential of CTAB-AuNRs at sublethal concentrations since genotoxic agents can induce carcinogenesis and/or heritable defects that may severely impact the health of an individual or the population.

3. Materials and Methods

3.1. **Reagents**

All chemicals used were of high purity or analytical grade. Dimethyl sulfoxide (DMSO; CAS no. 37-68-5), Triton X-100 (CAS no. 9002-93-1), low melting point (LMP) agarose (CAS no. 39346-81-1), Tris-HCl (CAS no. 1185-53-1), 30% (w/w) hydrogen peroxide (H_2O_2; CAS no. 7722-84-1) solution, 10 mg/mL ethidium bromide (CAS no 1239-45-8) solution and cetyltrimethylammonium bromide (CTAB; CAS no. 57-09-0) were purchased from Sigma-Aldrich (Madrid, Spain). Ethanol absolute (EtOH; CAS no. 64-17-5), sodium hydroxide (NaOH; CAS No. 1310-73-2), sodium chloride (NaCl; CAS no. 7647-14-5), hydrochloric acid (HCl, Cas no.7647-01-0) and Tris base (CAS no. 77-86-1) were bought from Merck (Darmstadt, Germany). Fetal bovine serum (FBS) and Molecular Probes® SYBR® Gold were purchased from Thermo Fisher Scientific (Madrid, Spain), while ethylenediaminetetraacetic acid disodium salt (Na_2EDTA; CAS no. 6381-92-6) and nitric acid (HNO_3; CAS no. 7697-37-2) were purchased from Prolab (Laval, Canada). Phosphate-buffered saline (PBS; CAS no. 10049-21-5) and normal melting point (NMP) agarose were supplied by Lonza (Basel, Swiss) and Bioline (London, UK), respectively. A gold pure calibration standard was obtained from Perkin Elmer (Waltham, MA, USA).

3.2. **Physicochemical characterization of the gold nanorods (AuNRs)**

CTAB-stabilized AuNRs (catalogue no. A12-10-750) with axial dimension=10 nm, long size dimension=35 nm and absorbance peak= 750 nm were supplied by Nanopartz™ (Salt Lake City, UT, USA) and stored according to manufacturer's recommendations. Size and morphology of the CTAB-AuNRs were assessed by Transmission Electron Microscopy (TEM) either in the stock or working suspensions using a Hitachi H-9000 microscope operated at 300 kV. For this analysis, a drop of the suspensions under study was placed on a carbon-coated copper grid and the solvent was left to evaporate at room temperature. Particle size distribution of CTAB-AuNRs was measured in 5 TEM images (30 AuNRs/image) using the ImageJ software (NIH, USA). To determine the crystallographic nature and purity of the tested AuNRs, a Hitachi H-9000 microscope equipped with x-ray diffraction mode and a spectrometer was used. Zeta potential was measured using a Zetasizer Nano ZS (Malvern Instruments, Worcestershire, UK). Measurements were performed in triplicate, either in distilled water or water from the Zebrafish facility (ZW).

3.3. Handling and preparation of the AuNRs suspensions

All procedures of handling and preparation of the CTAB-AuNRs suspensions were standardized to minimize within-experiment variations. The experiments were performed using the same batch of AuNRs. The stock suspension was kept at 4ºC, protected from light and remained stable without any detectable sign of precipitation or change of color throughout the study. Different concentrations of CTAB-AuNRs were freshly prepared from the stock suspension by direct dilution in autoclaved ZW.

3.4. Zebrafish (*Danio rerio*) maintenance and embryo collection

Danio rerio embryos used in this study were provided by the zebrafish facility established at the Department of Biology, University of Aveiro (Portugal). Adult zebrafish were maintained under standard controlled conditions (26.0 ± 1°C, 80% humidity, photoperiod cycle of 16 h light:8 h dark) in tanks equipped with recirculating systems. The fishes were fed with a commercially artificial diet (ZM 400 Granular), and maintained in carbon-filtered water with the following characteristics: 0.34 mg/L of Instant Ocean® synthetic sea salt (Spectrum Brands, USA), 26.0 ± 1°C, 750 ± 50 µS/cm, pH 7.5 ± 0.5 and dissolved oxygen saturation ≥ 95%.

For the experiments, zebrafish eggs were obtained by natural crossbreeding. Before the onset of darkness on the day prior to the test, zebrafish females and males were separated to guaranty that all the embryos will be in the same development stage and spawn traps (marbles) were deposited in the tanks to avoid the predation of the eggs by adult zebrafish. At the onset of light on the day of the test, zebrafish females and males were rejoined. Zebrafish eggs were carefully collected within 1 h after natural mating, rinsed in ZW and observed under a stereomicroscope (Stereoscopic Zoom MicroscopeSMZ 1500, Nikon Corporation, Japan). Unfertilized eggs, eggs with irregularities during cleavage and eggs with injuries or other kind of malformations were discarded.

3.5. Acute toxicity assessment

To assess the toxicity of CTAB-AuNRs on zebrafish embryos experiments were performed according to the OECD testing guideline 236 on Fish Embryo Acute Toxicity (FET) Test (OECD 2013). At 6 hours postfertilization (hpf) embryos were exposed to different concentrations of CTAB-AuNRs. A toxicity range finding test prior to the acute

toxicity definitive test was conducted to select the appropriate concentrations. The definitive study was conducted to determine the concentration producing 50% of mortality at 96 hpf ($LC_{50,96hpf}$). Lethality was therefore the first parameter to be evaluated. The embryo is considered dead if there is coagulation of the embryo, lack of somite formation after 48 h or lack of heart beat, which should be visible at 48 hpf. For the definitive test, embryos at 6 hpf were exposed to different concentrations of CTAB-AuNRs (50 to 150 µg/L) and CTAB (0.008 to 0.017 mM). Embryos exposed to ZW were used as negative controls. Ten embryos were used per replicate and 3 replicates were used per treatment, and distributed individually in 24-wells microplates (2 mL of test solution per well) containing 4 internal controls. Embryos were observed under a stereomicroscope (Stereoscopic Zoom MicroscopeSMZ 1500, Nikon Corporation, Japan) at 24, 48, 72 and 96 hpf and the following parameters were evaluated: survival, somite formation, incidence of pericardial edema, lack of heartbeat, malformations (general, spinal, tail and head), hatching, total body length (snout to tail tip) and developmental delay. At 48 hpf, the heart rate (beats/15 s) was measured by counting heart beats under a stereomicroscope in 3 randomly selected embryos of each replicate. The body length was measured in digital images taken from zebrafish embryos using the ImageJ software (NIH, USA). Development delay was obtained by matching the developmental stage of a given embryo with the developmental stages defined by Kimmel et al. (1995).

3.6. **Uptake of the AuNRs by zebrafish embryos**

To investigate the degree of uptake of CTAB-AuNRs, zebrafish embryos (6 hpf) were exposed to sublethal concentrations of the CTAB-AuNRs (42, 50, 60, 72 and 87 µg/L). For this analysis, 30 embryos/treatment were used and distributed individually in 24-wells microplates (2 mL of test solution per well). Three independent uptake experiments were performed. An aliquot (10 mL) of the incubation media was collected prior incubation. At the end of the exposure period (48 and 96 hpf), zebrafish embryos were rinsed twice in ZW to remove unspecific binding of AuNRs and weighted. The embryos were stored at -20°C until analysis.

AuNRs uptake by zebrafish embryos was estimated based on embryo Au content quantified by Inductively Coupled Plasma-Optical Emission Spectrometry (ICP-OES). The collected samples were transferred into polytetrafluoroethylene (PTFE) vessels and digested in a mixture of 1 mL aqua regia (3 HCl:1 HNO_3), 1 mL 30% H_2O_2 and 6 mL deionized water for 1.5 h at 220 °C, 4 bar, 1200 watts using an Ethos Advanced Microwave Digestion System (Milestone, Bergamo, Italy). After cooling, the

samples were diluted in deionized water to a final volume of 6 mL. To estimate the digestion and recovery efficiency of Au, embryos and ZW samples were spiked with different concentrations (12.5, 25 and 50 µg/L) of Au or AuNRs.

Samples were injected in an iCAP 7000 ICP optical emission spectrometer (Thermo Fisher Scientific, Cambridge, England) equipped with an CETAC ASX520 autosampler and total elemental Au quantified (axial mode, wavelength 242.795, exposure time 15 s) using an eight-point standard curve (1.65 to 200 µg/L). Data are expressed as µg Au/g fresh weight.

3.7. **Genotoxicity assessment**

Single cell gel electrophoresis assay (Comet assay) was performed to assess the ability of AuNRs to cause DNA damage in zebrafish embryos. The concept of this method is to visualize migration of DNA strands from individual agarose-embedded cells. If there is DNA damage, the DNA supercoils are relaxed and single-strand breaks will therefore be able to migrate during electrophoresis, creating a comet whose head contains the high-molecular-weight DNA and tail contains the migrated DNA fragments. Tail intensity and tail moment are two forms of expressing the DNA damage in individual cells. Tail intensity is the percentage of DNA in the tail, whereas tail moment is the percent DNA in the tail multiplied by the distance between the means of the head and tail distributions (Olive and Banath 2006).

For this analysis, 25 embryos (6 hpf) were used and distributed individually in 24-wells microplates (2 mL of test solution per well). Zebrafish embryos were exposed to subtoxic concentrations of CTAB-AuNRs (72, 87 and 104 µg/L). Embryos exposed to 100 mM of H_2O_2 for 10 min were used as a positive control.

Embryo cells were isolated as previously described (Kosmehl, Hallare et al. 2006) with some modifications. Briefly, at the end of the exposure period (48 or 96 hpf), zebrafish embryos were rinsed with PBS pH 7.4, transferred to flat microcentrifuge tubes and gently homogenized in 100 µL of PBS pH 7.4 with a pestle. The cell suspensions were then filtered through a 70 µm strainer in order to separate the individual cells from the remaining macerated tissues and centrifuged at 300 × *g*, 5 min, 4ºC. The pellets were resuspended in 200 µL of ice-cold freezing medium (FBS with 10% DMSO), placed at -20 ºC for 3 h and then stored at -80 ºC until analysis.

The comet assay was carried out under alkaline conditions following the procedure developed by Singh et al. with some modifications(Singh, McCoy et al. 1988). Briefly, cell suspensions were thawed, centrifuged at 300 × *g*, 5 min, 4 ºC and

the resulting pellets resuspended in PBS pH 7.4. The cell suspensions were subjected to another centrifugation at 400 × *g*, 5 min, 4 ºC. The resulting pellets were gently mixed in 100 µL of 1% (w/v) LMP agarose and layered onto dry microscope slides (VWR, Darmstadt, Germany) pre-coated with 1% NMP agarose. After gel solidification at 4 ºC, the slides were placed in a coplin jar and immersed in ice-cold lysis solution (2.5 M NaCl, 100 mM Na_2EDTA, 10 mM Tris-base, 10 M NaOH, pH 10, supplemented with 1%Triton-X 100 and 10% DMSO) during 1.5 h at 4 ºC and protected from light to lyse the cells and separate DNA from histones. For unwinding of DNA, all slides were immersed in freshly prepared electrophoresis buffer (200 mM Na_2EDTA, 0.3 M NaOH pH>13) in the electrophoresis unit for 20 min at 4 ºC, followed by electrophoresis for 15 min at 25 V and 300 mA. The slides were then neutralized with 0.4M Tris base pH 7.5 followed by fixation with EtOH 70% and 96% for 15 min each at room temperature. After air-drying the slides overnight, DNA was stained with a 20 µg/mL ethidium bromide solution. The slides were coded, and one scorer performed the comet analysis using a fluorescence microscope (Nikon Eclipse E400 microscope attached to an epifluorescence illuminator Nikon C-SHG1) with 500x magnification and the image analysis software Comet Assay IV (Perceptive Instruments, Suffolk, UK). The percentage of DNA in the comet tail and the olive tail moment were used as a measure of the amount of DNA damage. A hundred cells per slide (50 for each replicate gel) were counted and three independent experiments were performed in triplicate.

3.8. **Statistical Analysis**

Data are expressed as mean± standard error of the mean (SEM). Statistical and nonlinear regression analyses were performed using the GraphPad Prism 6 software (La Jolla, CA, USA). Median lethal concentration ($LC_{50,96h}$) was calculated by fitting concentration-response curves with cumulative mortality obtained after 96 h of exposure to CTAB-AuNRs. Parametric analyszes were performed using one-way ANOVA with Dunnett's post hoc test for multiple comparisons. Non-parametric analysis of genotoxicity data was performed using Kruskal-Wallis followed by post-hoc Dunn's test for multiple comparisons. Significance was accepted at a P value <0.05.

4. Results

4.1. **Physicochemical characterization of CTAB-AuNRs**

The main characteristics of the CTAB-AuNRs stock suspension used in this study are summarized in **Figure 4, Figure 5** and **Table 1**. TEM analysis revealed high monodispersity and well-defined rod-like shape of tested AuNRs (**Figure 4A** and **B**). The EDX spectrum depicted in **Figure 5A** confirms the purity of the stock suspension under evaluation as only peaks of Au and copper, the latter resulting from the copper grid, were detected. **Figure 5B** shows the X-ray diffraction pattern of AuNRs, which is consistent with metallic Au. The average length and diameter measured by TEM was 19.982 ± 0.462 nm and 7.407 ± 0.110 nm (**Figure 4**), respectively, while the zeta potential measured by DLS was 69.9 ± 14.8 mV (**Table 1**).

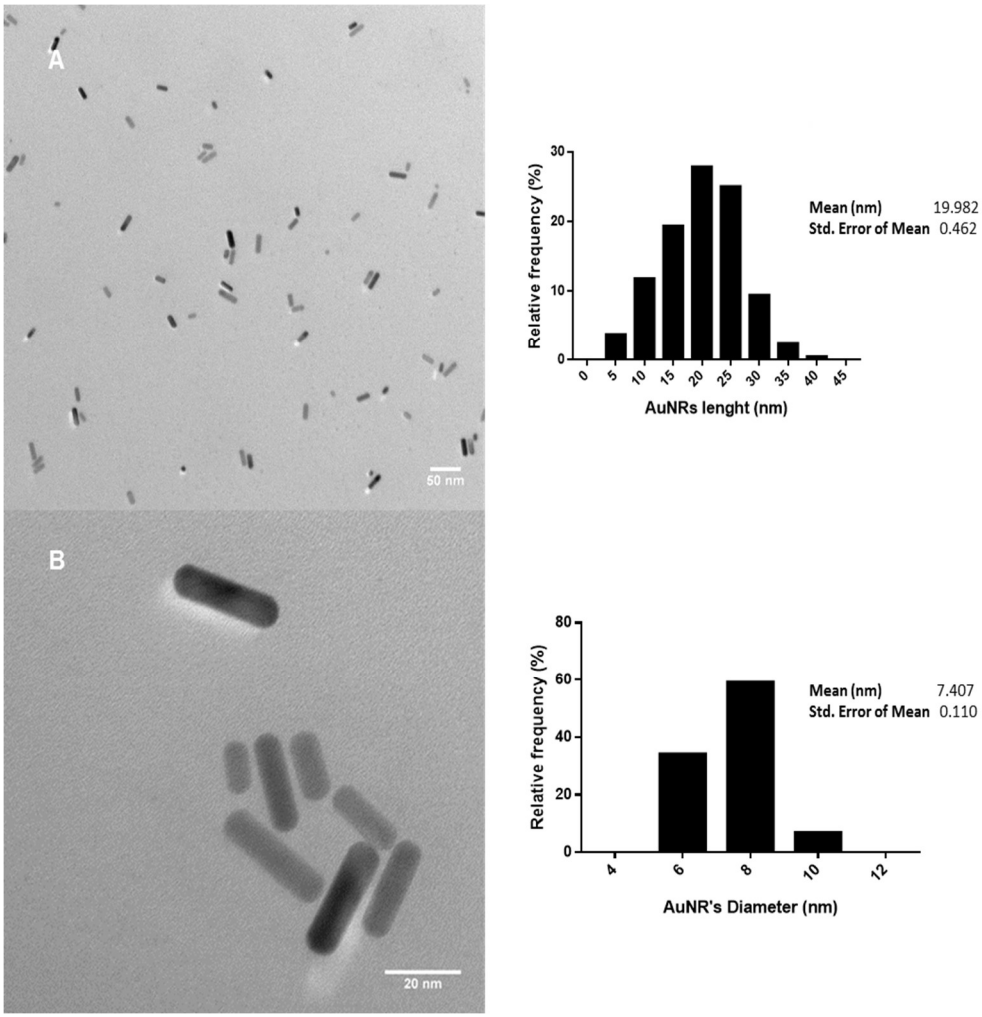

Figure 4 Representative TEM micrographs of the CTAB-AuNRs stock suspension with magnification of 30000x (A) and 200000x (B) and the corresponding histograms of size distribution. Scale bars: 50 nm (A) and 20 nm (B).

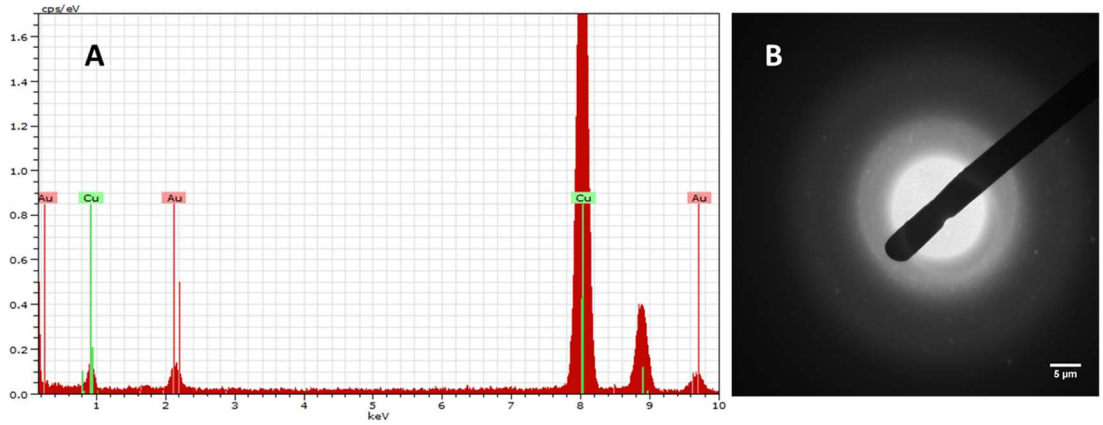

Figure 5 EDX spectrum (A) and X-ray pattern (B) of the CTAB-AuNRs stock suspension. Scale bar: 5 µm (B).

Comparing the physicochemical characterization data of CTAB-AuNRs obtained in this study with the values provided by the manufacturer some differences were detected, a small reduction in the Au concentration of the stock suspension and in size (length and diameter) of the CTAB-AuNRs and an increase in the zeta potential were observed, as shown in **Table 1**.

Table 1 Summary of the main physicochemical features of the tested AuNRs dispersed in water.

	Manufacturer's Measurements	**Performed Measurements**
Length (nm)[a)]	35	20.0 ± 0.46
Diameter (nm)[a)]	10	7.4 ± 0.11
Zeta Potential (mV)[b)]	40	69.9 ± 14.8
Concentration (µg/L)[c)]	35	24

a) Dimensions (length and diameter) were determined by TEM. Results are expressed as mean ± SD.
b) Zeta potential was determined by DLS. Results are expressed as mean ± SEM.
c) Concentration of Au in the colloidal suspensions was determined by ICP-OES.

To evaluate how the dispersion of CTAB-AuNRs in ZW influenced the characteristics of these commercial NMs, TEM analysis and zeta potential measurements of the working suspensions were performed. The TEM analysis of CTAB-AuNRs after dispersion in ZW (**Figure 6**) demonstrated that there was agglomeration of the AuNRs in ZW, particularly at high concentrations such as 104 µg/L (**Figure 6A**) and 150 µg/L (**Figure 6B**), when compared to the highly monodispersed AuNRs stock suspension (**Figure 4A**). As presented in **Table 2**, the

dispersion of CTAB-AuNRs in ZW caused a reversion in their original electrostatic potential from positive to negative at all concentrations tested, with values ranging from -2.8 to -26.2 mV.

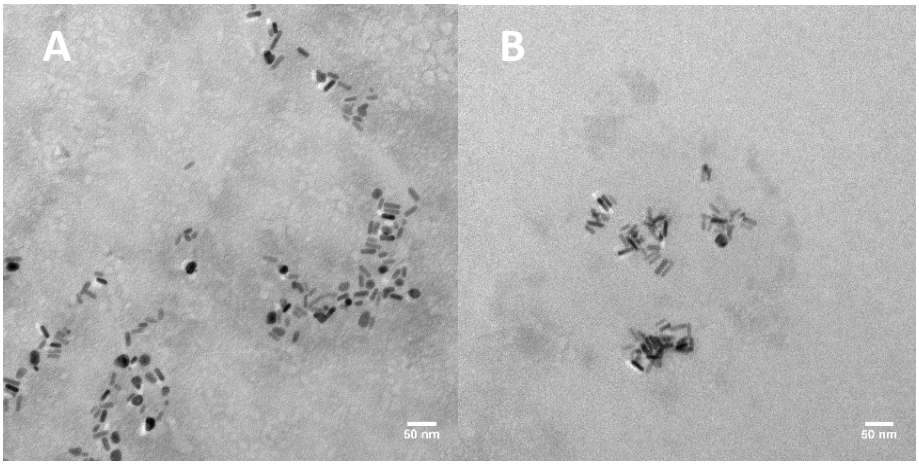

Figure 6 Representative TEM micrographs of the CTAB-AuNRs working suspensions dispersed in zebrafish water (ZW) at 104 µg/L (A) and 150 µg/L (B) with magnification of 60000x Scale bars: 50 nm (A and B).

Table 2 Zeta potential of the stock suspension of CTAB-AuNRs and working suspensions in ZW.

[CTAB-AuNRs] (µg/L)	Zeta Potential (mV)
35000 (Stock)	69.9 ± 14.8
60	−23.0 ± 2.2
72	−26.2 ± 2.2
87	−2.8 ± 4.6
104	−4.3 ± 2.7
125	−23.0 ± 3.8
150	−14.6 ± 3.0

Values are mean ± SEM.

4.2. **Lethality and developmental effects of CTAB-AuNRs on zebrafish embryos**

The potential adverse effects to zebrafish embryos caused by CTAB-AuNRs exposure was investigated following the OECD TG 236. A preliminary range finding test showed 100% of mortality in zebrafish embryos exposed to CTAB-AuNRs concentrations ≥ 185 µg/L at 24 hpf (data not shown). According to these findings, a definitive test was performed at a lower concentration range (50, 60, 72, 87, 104, 125

and 150 µg/L). As shown in **Figure 7**, 6 hpf embryos exposed to the CTAB-AuNR's highest tested concentrations (125 and 150 µg/L) exhibited a significant mortality rate at 24 hpf, which was around, 67% and 73%, respectively. At 96 hpf, the cumulative mortality rate increased to 100%. Moreover, at the other concentrations tested, the cumulative mortality at 96 hpf was found to be ≤10%. Analysis of the concentration-response curves with cumulative mortality at 96 hpf revealed a median lethal concentration ($LC_{50,96h}$) of 110.2 µg/L (95% confidence interval 100.6 – 122.8 µg/L).

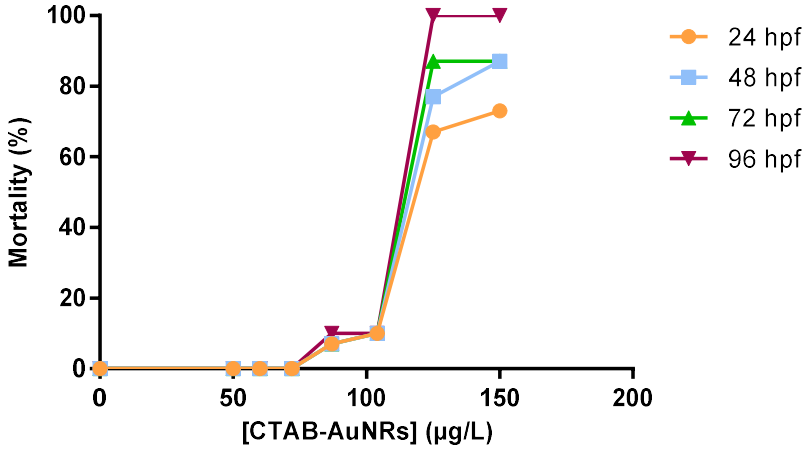

Figure 7 Zebrafish embryos mortality at different time-points (24, 48, 72 and 96 hpf) following exposure to CTAB-AuNRs (n=30).

The effects of CTAB-AuNRs on the developmental parameters of zebrafish embryos throughout the exposure period are summarized in **Table 3** and **Table 4**, and **Figure 8**. At 24 hpf, detachment of the tail, formation of somites and the eye and brain anlage were visible in the control (non-exposed) zebrafish embryos (**Figure 8A**), as expected. Moreover, embryos exposed to concentrations of CTAB-AuNRs between 50 and 87 µg/L did not show any alteration in these morphological structures. On the other hand, CTAB-AuNRs at 104, 125 and 150 µg/L induced several developmental anomalies in exposed embryos, namely abnormal eye and head development, tail deformities (e.g. neither posterior elongation of the yolk sac to form the yolk extension nor elongation of the tail bud), abnormal yolk sac and edema (**Table 3** and **Figure 8**).

The onset of pigmentation in the eyes and body of zebrafish embryos normally occurs between 24 and 48 hpf, however 26%, 86% and 75% of the embryos exposed to 104 (**Figure 8F**), 125 (**Figure 8G**) and 150 µg/L (**Figure 8H**) of CTAB-AuNRs, respectively, shown decreased pigmentation when compared with the controls (**Figure 8E**). At 48 hpf, the heart rate was measured and the results are listed in **Table 4**. Embryos exposed to CTAB-AuNRs concentrations ≤104 µg/L suffered no significant

variations in this parameter when compared to the control group, while at the highest concentrations it was observed a clear reduction in the heart rate of the few embryos alive (data not shown). In addition, anomalies in other developmental parameters such as hatching rate, which ensues between 48 and 72 hpf, swim bladder inflation, protrusion of the mouth and pectoral fin formation were not detected.

As depicted in **Figure 8** the developmental abnormalities detected at 24 and 48 hpf were more severe in embryos exposed to 125 and 150 µg/L (**Figure 8C**, **G** and **D**, **H**, respectively) than in embryos exposed to 104 µg/L of CTAB-AuNRs (**Figure 8B** and **F**). In fact, all embryos exposed to the two highest concentrations ultimately died within the period of exposure (**Figure 8L**), whereas for the embryos exposed to 104 µg/L some of the alterations detected at 24 and 48 hpf, such as abnormal eye and head and hypopigmentation, were not observed at 96 hpf as represented in the chronological sequence of **Figure 8B**, **F** and **J**, which represents the same individual at 24, 48 and 96 hpf, respectively. Thus, it seems that CTAB-AuNRs exposure delayed the development of the eyes and brain, the elongation of the tail and the onset of pigmentation. Nevertheless, 22% of the zebrafish embryos exposed to 104 µg/L still displayed pericardial edema and/or tail deformities at 96 hpf (**Figure 8J** and **K**). Furthermore, a reduction of zebrafish's body length corresponding to a maximum effect of 6% was detected following exposure to 72, 87 and 104 µg/L. However, this increase was statistically significant only in zebrafish exposed to 72 and 104 µg/L of CTAB-AuNRs compared with the control group (**Table 4**). Overall, CTAB-AuNRs induced an all-or-nothing effect on zebrafish embryos, which did not exhibit severe malformations at sublethal concentrations.

The AuNRs tested are capped with CTAB, which has been proved to be a highly toxic surfactant. Since CTAB is present in the stock suspension at a considerable concentration (4 mM), both adsorbed to the surface of AuNRs and freely dispersed in solution, it was mandatory to verify if the toxicity observed in the exposed zebrafish embryos was due to this compound. Therefore, zebrafish embryos were exposed to CTAB solutions with the same concentrations present in the tested CTAB-AuNRs dispersions (0.008, 0.010, 0.012, 0.014 and 0.017 mM). For all tested concentrations, CTAB induced 100% mortality within 30 min after exposure. As illustrated in **Figure 9B**, the membranes of the exposed-embryos were rapidly disrupted in the presence of CTAB, causing their coagulation. Hence, CTAB itself may account for the acute toxicity observed in embryos subjected to CTAB-AuNRs treatment.

Table 3 Effects of CTAB-AuNRs on the developmental parameters of zebrafish embryos (n=1).

[CTAB-AuNRs] (µg/L)	Alterations (%) at 24 hpf				Alterations (%) at 48 hpf	Malformations (%) at 96 hpf	
	Abnormal eye/ head	Abnormal tail	Abnormal Yolk Sac	Edema	Hypopigmentation	Pericardial edema	Tail deformity
Control	0	0	0	0	0	0	0
50	0	0	0	0	0	0	0
60	0	0	0	0	0	0	0
72	0	0	0	0	0	3.33	3.33
87	0	0	3.3	0	0	0	0
104	30	22.2	41	22	26	11.11	14.8
125	70	90	70	30	86	*	*
150	75	75	63	13	75	*	*

* All exposed embryos were dead at 96 hpf.

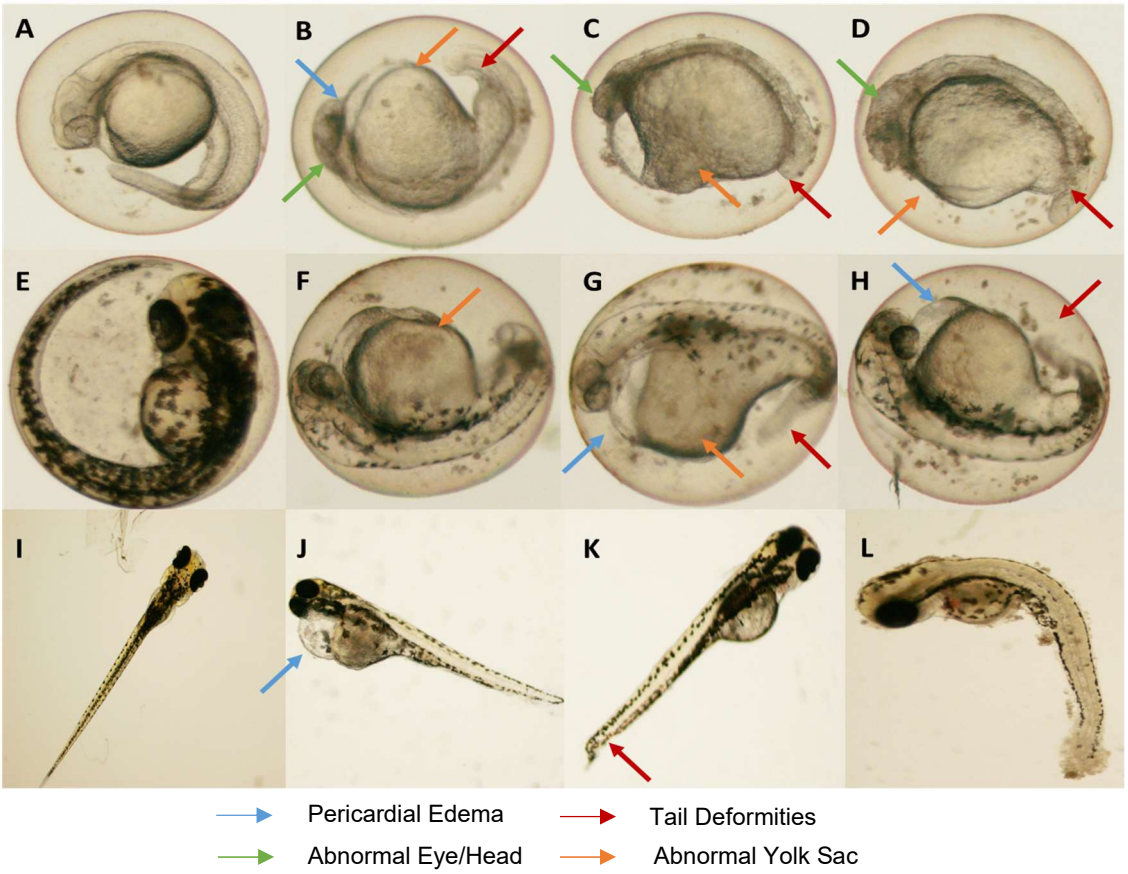

Figure 8 Zebrafish embryos abnormalities during exposure to CTAB-AuNRs. At 24 hpf: Control embryos (**A**) and embryos exposed to 104 µg/L (**B**), 125 µg/L (**C**) and 150 µg/L (**D**). At 48 hpf: control embryos (**E**) and embryos exposed to 104 µg/L (**F**), 125 µg/L (**G**) and 150 µg/L (**H**). At 96 hpf: Control embryos (**I**) and embryos exposed to 104 µg/L (**J** and **K**). Dead embryo at 96 hpf (**L**).

Table 4 Effects of CTAB-AuNRs exposure on zebrafish's heart rate (measured at 48 hpf) and body length (measured at 96 hpf).

[CTAB-AuNR] (µg/L)	Heart rate (beats/min) at 48hpf	Body Length (mm) at 96 hpf
Control	172.9 ± 2.2	3.80 ± 0.032
50	167.1 ± 3.0	3.80 ± 0.023
60	175.1 ± 2.0	3.79 ± 0.032
72	172.9 ± 2.0	3.63 ± 0.030 *
87	175.6 ± 2.0	3.71 ± 0.035
104	159.0 ± 3.4	3.56 ± 0.036 **

Values are mean ± SEM. Data was analyzed by one-way analysis of variance (ANOVA) followed by Dunnett's post hoc test (* p <0.001 and ** p<0.0001 vs control).

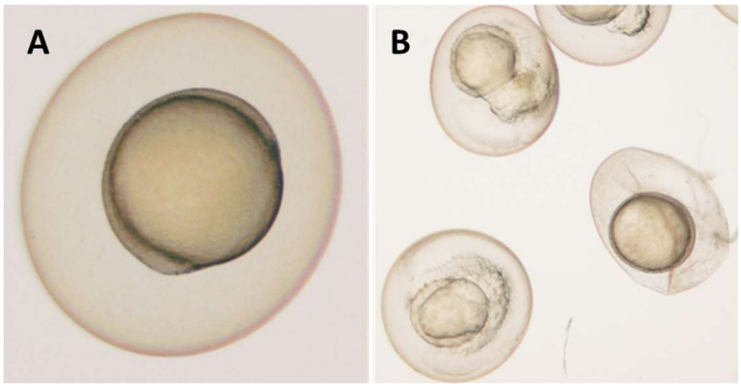

Figure 9 Effects of CTAB solutions in 6 hpf embryos. Micrographs of control (non-exposed) (A) and exposed to 0.017 mM CTAB (B), which corresponds to the CTAB content present at the highest concentration of CTAB-AuNRs tested (150 µg/L).

4.3. **Uptake of the AuNRs by the zebrafish embryos**

The uptake of CTAB-AuNRs was estimated in zebrafish embryos exposed to 42, 50, 60, 72 and 87 µg/L at 48 and 96 hpf by ICP-OES. The analysis of the Au content with ICP-OES required previous digestion of the samples. Therefore, to evaluate the digestion and the recovery efficiency of the Au with the selected protocol (220 ºC, 5 bar and 1h30min), embryos and ZW samples were spiked with different concentrations (12.5, 25 and 50 µg/L) of Au or AuNRs. As shown in **Table 5**, the recovery efficiency was optimal for both embryo and ZW samples with Au or AuNRs, which indicates that the digestion procedure was effective and no significant loss of elemental Au occurred throughout the process until sample injection.

The Au embryo content was determined against an eight-point calibration curve (**Figure 10**). As represented in **Figure 11**, elemental Au was detected in zebrafish embryos exposed to CTAB-AuNRs both at 48 and 96 hpf, with values ranging from 0.24 ± 0.06 to 1.02 ± 0.27 µg/g fresh weight and from 0.02±0.02 to 2.41±0.77 µg/g fresh weight, respectively. Both at 48 and 96 hpf, the accumulation of Au in zebrafish embryos was concentration-dependent. Taking into account the initial administered concentration of CTAB-AuNRs, the uptake of CTAB-AuNRs at 48 and 96 hpf was similar and always inferior to 0.6% (**Table 6**). Elemental Au was not detected in the control samples (i.e. non-exposed zebrafish embryos) as expected (data not shown).

Table 5 Recovery efficiency of Au in zebrafish embryos (ZF) and zebrafish water (ZW) samples spiked with different concentrations (12.5, 25 and 50 µg/L) of Au or AuNRs as assessed by ICP-OES.

Sample	Recovery Efficiency (%)
Au Standard at 12.5 µg/L with ZF	100.19 ± 1.32
Au Standard at 25 µg/L with ZF	100.20 ± 0.27
Au Standard at 50 µg/L with ZF	101.14 ± 0.22
AuNRs at 12.5 µg/L with ZF	123.49 ± 3.78
AuNRs at 25 µg/L with ZF	114.31 ± 0.62
AuNRs at 50 µg/L with ZF	104.72 ± 0.04
Au Standard at 12.5 µg/L in ZW	100.93 ± 0.85
Au Standard at 25 µg/L in ZW	94.78 ± 1.24
Au Standard at 50 µg/L in ZW	95.71 ± 0.25
AuNRs at 12.5 µg/L in ZW	139.15 ± 9.96
AuNRs at 25 µg/L in ZW	104.73 ± 3.46
AuNRs at 50 µg/L in ZW	102.00 ± 6.91

Values are mean ± SEM.

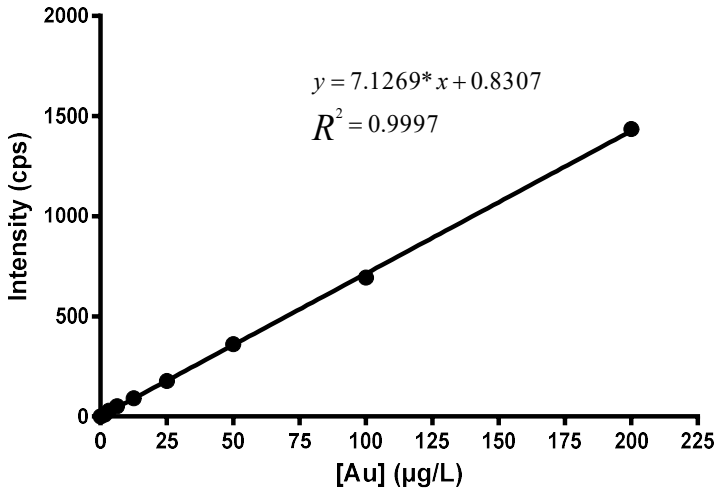

Figure 10 Representative eight-point (0-200 µg/L) calibration curve used for Au content analysis by ICP-OES.

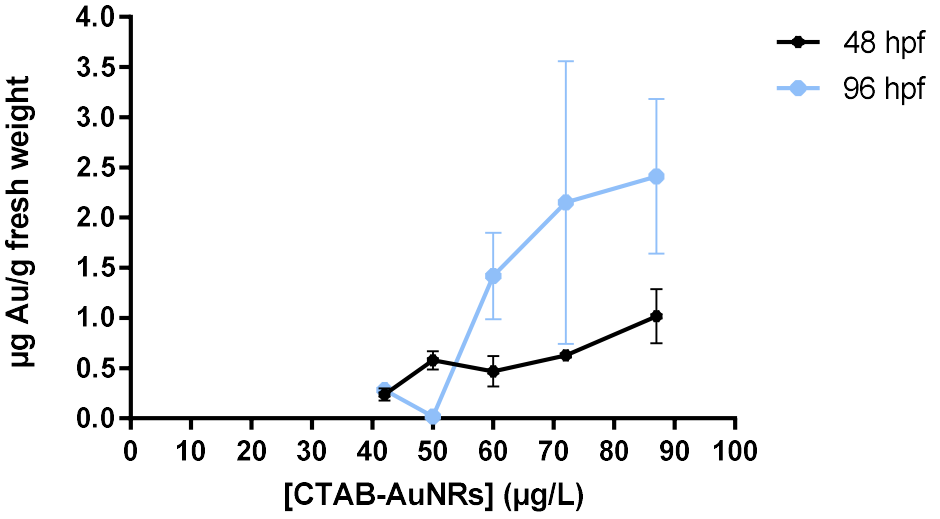

Figure 11 Au content of embryos exposed to different concentrations of CTAB-AuNRs at 48 and 96 hpf quantified by ICP-OES and expressed as µg Au/g fresh weight.

Table 6 Fraction of elemental gold in zebrafish tissues comparing to the initial concentration of CTAB-AuNRs in media expressed as percentage (%) of uptake.

[CTAB-AuNRs] (µg/L)	Uptake (%)	
	48 hpf	96hpf
42	0.29 ± 0.11	0.13 ± 0.08
50	0.55 ± 0.04	0.01 ± 0.01
60	0.26 ± 0.05	0.40 ± 0.10
72	0.51 ± 0.17	0.44 ± 0.30
87	0.49 ± 0.16	0.49 ± 0.22

Data represents the mean ± SEM of three independent experiments (n = 3 per group).

4.4. **Genotoxicity assessment**

The genotoxic potential of CTAB-AuNRs was assessed by the Comet assay. As represented in **Table 7**, exposure of early life stages of zebrafish (6 hpf) to CTAB-AuNRs did not induce significant DNA damage at 48 and 96 hpf. Although embryos exposed to 72 and 87 µg/L showed a slightly increase in tail intensity and tail moment at 48 hpf, there is no significant difference when compared to the control group. Zebrafish embryos exposed to 100 mM H_2O_2 for 10 minutes (positive control) exhibited a significant DNA damage (tail intensity and tail moment values were 83% and 21, respectively).

Table 7 Comet assay analysis of DNA damage in zebrafish embryos exposed to different concentrations of CTAB-AuNRs at 48 and 96 hpf.

	Tail Intensity (%)	**Tail Moment**
48 hpf		
Control	13.17 ± 1.01	1.30 ± 0.126
72 µg/L	15.39 ± 5.17	1.66 ± 0.604
87 µg/L	17.04 ± 1.14	1.72 ± 0.231
104 µg/L	12.88 ± 2.40	1.25 ± 0.238
96 hpf		
Control	11.24 ± 1.81	1.10 ± 0.232
72 µg/L	11.43 ± 2.40	0.98 ± 0.219
87 µg/L	10.94 ± 1.51	0.96 ± 0.152
104 µg/L	11.61 ± 1.17	1.14 ± 0.041

Data represents the mean ± SEM of three independent experiments (n = 3 per group).

5. Discussion

The physicochemical characterization of NMs is an important step in toxicity assessment as their behavior in the media (e.g. aggregation, sedimentation) and their interaction with the biological systems are highly dependent on their chemical composition, surface chemistry, particle size, shape, charge and dispersion stability. Hence, in order to correlate NM's characteristics with their biological/toxicological induced responses as well as to provide a reference for comparison with other studies, physicochemical characterization of CTAB-AuNRs was performed. The CTAB-AuNRs stock suspension used in this study was highly monodispersed and the AuNRs had an average length and diameter of 19.982 nm and 7.407 nm, respectively, and a zeta potential of 69 mV. The positively charged CTAB adsorbed on AuNRs surface is responsible for the high positive electrostatic potential shown by the AuNRs stock suspension. This coating creates mutual repulsions and, therefore prevents the agglomeration of AuNRs. Comparing our data with the characteristics provided by the manufacturer, there is a slightly difference in all the parameters measured. Commercial NMs suspensions can suffer degradation and/or alteration of their properties specially if they contain organic compounds, which highlights even more the need for a complete characterization, a step that is not always conducted in (eco)toxicological studies that rely on the manufacturer's analysis. The characterization of CTAB-AuNRs in the dispersion media (ZW) was also performed and a shift of the surface charge from positive to negative, with values ranging from -2.8 to -26.2 mV, was detected. Zeta potential is a measure of the stability of colloidal suspensions, and particles with zeta potential higher than +30 mV or lower than -30 mV are normally considered stable. This parameter is highly dependent on the physicochemical properties of the dispersion media such as ionic strength, ionic composition and pH. Hence, the high ionic strength of the ZW (conductivity = 750 µS/cm) may impart high instability to CTAB-AuNRs dispersions resulting in the formation of agglomerates/aggregates. TEM analysis of CTAB-AuNRs after dispersion in ZW confirmed the agglomeration of the AuNRs in ZW. The aggregation of CTAB-AuNRs can affect their bioavailability and uptake to zebrafish embryos and consequently result in different toxicological responses. Aggregation-dependent toxicity has been seen in many studies. For instance, the toxicity of TiO_2 NMs towards zebrafish has been shown to decline in exposure media with higher ionic strength, since it increases the aggregation of this type NM and thus decrease its bioavailability (Fang, Yu et al. 2015).

Following characterization, early life stages of zebrafish were treated with concentrations between 50 and 150 µg/L of CTAB-AuNRs, and lethality and effects on embryonic development were analyzed. Under our experimental conditions, the LC_{50}

value obtained for CTAB-AuNRs was 110.2 µg/L. This value was found to be higher than the obtained for the same CTAB-AuNRs in neonates of two species of cladocerans (*Daphnia magna* and *Daphnia longispina,* 3.39 and 4.43 µg/L, respectively) and for *Brachionus calyciflorus (*51 µg/L) (Galindo 2014). These findings support the view that different species exhibit specific sensitivity when exposed to the very same NMs. For instance, *Daphnia magna* has been shown to be more tolerant to Ag-NMs than *Daphnia pulex* or *Daphnia galeata* (Völker, Boedicker et al. 2013).

Regarding, the effects of CTAB-AuNRs on the development of zebrafish embryos, it was observed an all-or-nothing response as only the embryos exposed to the highest sublethal concentration tested (104 µg/L) have shown development anomalies, including pericardial edema and tail deformities. However, the incidence of these alterations was 22%. A delay in the development of head and eyes, elongation of the tail and in the onset of pigmentation was also detected, which could result from an impairment of the cellular processes that take place during gastrula and segmentation periods. While it seems that this delay was recoverable at 96 hpf, we cannot exclude that the initial retardation in embryo development will have repercussions later on. The CTAB-AuNRs might be able to induce a cascade of alterations, namely brain dysfunction, which may not be detected structurally or functionally until much later in life. Furthermore, the zebrafish embryos exposed to 72, 87 and 104 µg/L of CTAB-AuNRs revealed a reduction of body size, although only significant for 72 and 104 µg/L compared with the control group, which further supports the idea of delayed development induced by CTAB-AuNRs. The reduction of zebrafish's body size can have severe implications as it might increase the susceptibility to predation, disrupt feeding behavior, reduce the reproductive success and thus reduce the fitness of the individual or the population (Peters 1986, Uusi-Heikkilä, Kuparinen et al. 2012). Overall, it would be interesting to further assess for adverse effects in juvenile and/or adult stages of zebrafish exposed to sublethal concentrations of CTAB-AuNRs, namely by examining locomotor activity, predator/prey interactions and reproductive and social behaviors. Meanwhile, adverse effects caused by CTAB-AuNRs were also reported for other organisms. Four cladocerans species have shown reduced body length when exposed to CTAB-AuNRs at concentrations ranging from 1.41 to 18.1 µg/L (Galindo 2014), whereas white-rot fugi exhibited growth inhibition at concentrations between 15.91 to 33 mg/L (Galindo, Pereira et al. 2013). Most of the studies employing zebrafish embryos for toxicity assessment of AuNMs have been focused in sphere-shaped and no evident toxicity has been reported. For instance, Browning et al. have

demonstrated that spherical AuNMs (86.2 nm) did not cause significant mortality or malformations at concentrations up to 78 µg/Ml (Browning, Huang et al. 2013).

The CTAB is the most employed surfactant for the synthesis of AuNRs as it guides the growth of Au seeds into rod-like shape and efficiently prevents their aggregation by adsorbing to their surface. However, CTAB is a highly toxic cationic surfactant and although several methods are employed to purify the final AuNRs suspension, some free CTAB might remain. Therefore, to test whether the CTAB both adsorbed to the surface of AuNRs and freely dispersed in solution was responsible for the toxicity induced by CTAB-AuNRs, zebrafish embryos were treated with solutions of pure CTAB at the same concentrations present in the CTAB-AuNRs working suspensions. CTAB provoked 100% mortality within 30 min of exposure for all concentrations tested. This comes with no surprise as this surfactant was shown to cause 50% lethality in exposed *Daphnia magna* at 0.16 µM (Sandbacka, Christianson et al. 2000), which is much lower than the concentrations tested in our study (8 – 17 µM). Hence, CTAB itself may account for the acute toxicity observed in embryos subjected to CTAB-AuNRs treatment. Alkilany et al. found that either CTAB-AuNRs dispersions or CTAB-containing supernatant resulting from centrifugation of the CTAB-AuNRs dispersions induced similar toxicity in a human colon cancer cell line, HT-29 (Alkilany, Nagaria et al. 2009). Moreover, CTAB-AuNRs and free CTAB have also been reported to cause similar mortality in *Daphnia magna* (Bozich, Lohse et al. 2014). In the present study, pure CTAB caused a much more pronounced lethality of zebrafish embryos than CTAB-AuNRs at the same concentrations. Therefore, it can be hypothesized that the concentration of CTAB present in the CTAB-AuNRs stock suspension was actually inferior than the one provided by the manufacturer, possibly due to its degradation, or the AuNRs exerted a protective function by reducing the bioavailability of free CTAB and therefore delaying its toxicity. The latter hypothesis highlights the potential of AuNRs to be employed for water remediation by removing pollutants such as metal species, organic dyes and pharmaceuticals. Nevertheless, to clearly discriminate the contribution of each component, i.e CTAB and AuNRs for the toxicity induced by the CTAB-AuNRs, it would be necessary to test bare AuNRs with the same size and shape as those of the AuNRs tested and compare the response induced in zebrafish embryos.

To investigated whether or not CTAB-AuNRs were internalized by exposed zebrafish embryos and if it had some association with the toxicity observed, the Au content of zebrafish embryos was measured. The CTAB-AuNRs were indeed internalized in a concentration dependent-manner. Therefore, the negative electrostatic

potential of CTAB-AuNRs in ZW did not hamper their internalization by the negatively charged cellular membrane. The higher Au content per g of fresh weight detected at 96 hpf results essentially from the higher weight of zebrafish embryos at 48 hpf as they are still protected by the chorion. The % of uptake, in other words, the fraction of elemental Au in zebrafish tissues comparing to the initial concentration of CTAB-AuNRs in the incubation media is therefore a better parameter to compare the internalization between the two time points. The uptake of CTAB-AuNRs by zebrafish embryos was similar at 48 and 96 hpf but less than 1%, which might have resulted from the aggregation of CTAB-AuNRs in ZW. The similar internalization level verified before (48 hpf) and after hatching (96 hpf), particularly for the highest tested concentrations (60 – 87 µg/L), raises two hypotheses: the CTAB-AuNRs surpassed the chorion and were internalized by the embryos within the first 48 hpf or in alternative the Au measured at 48 hpf was due to CTAB-AuNRs adsorbed to the chorion and the accumulation of AuNRs only occurred after hatching. The lethal effect of CTAB-AuNRs on zebrafish embryos was mostly established within 24 hpf, which supports the former hypothesis, considering the toxicity observed is related with the accumulation of CTAB-AuNRs. In fact, AuNPs have been reported to diffuse through the chorionic pore canals and reach the inner cell mass of zebrafish embryos, remaining inside them throughout the entire development (Browning, Lee et al. 2009, Browning, Huang et al. 2013). However, the second hypothesis is also plausible as the adsorption of CTAB-AuNRs to the chorion may hamper gas exchange (oxygen supply) and osmoregulation, both essential for the development of the zebrafish embryos. In line with our results, Wang et al. have also observed an “all-or-nothing” effect in zebrafish embryos exposed to sublethal doses of CTAB-AuNRs, with no visible malformations (Wang, Xie et al. 2016). However, they reported a higher uptake of Au by zebrafish embryos at 8 hpf (≈20%) comparing to 80 hpf (≈5%), which better sustain the later theory. In our study, healthy embryos - with no visible phenotypic defects after CTAB-AuNRs exposure - were able to accumulate Au in their tissues, although in a low % (less than 1%). This finding brings into question if long term deposition of AuNRs in the embryo can induce toxicity in subsequent life stages. Asharani et al. have also reported that hatched zebrafish embryos exposed to 25 and 50 µg/mL of spherical AuNMs accumulated these NMs in a small percentage, approximately between 2 and 3%. However, no toxicity was detected towards zebrafish embryos (Asharani, Lianwu et al. 2011). The uptake of CTAB-AuNRs have been also demonstrated to occur in *Daphnia magna*, a low-trophic-level organism. This raises further concerns of potential transfer and magnification in food webs as have been already reported for spherical AuNMs which were detected in *Daphnia magna* fed with the unicellular microorganisms *Chlamydomonas reinhardtii*

and *Euglena gracilis* previously exposed to these NMs (Lee, Yoon et al. 2015), and also for TiO_2NMs transferred from *Daphnia magna* to zebrafish by dietary exposure (Zhu, Wang et al. 2010).

DNA damage can induce carcinogenesis and/or heritable defects that severely impact the health of an individual or the population. Additionally, genotoxic alterations induced by NMs are being considered as potential biomarker of susceptibility. Hence, the possibility of CTAB-AuNRs to act as a genotoxic agent was investigated. No DNA damage was detected in zebrafish embryo cells both at 48 and 96 hfp, however the long-term accumulation of CTAB-AuNRs might elicit genotoxic events. Thus further research on this topic must be conducted. Previous studies focused on the genotoxicity of AuNMs have reported no detrimental effects on DNA of exposed rodents. For instance, Downs et al. showed accumulation of spherical AuNMs of different sizes (2, 20, 200 nm) in the liver and lung tissues of rats exposed through IV injection to 0.030 mg/kg bw (Downs, Crosby et al. 2012). However, this tissue accumulation was neither translated into an increase in DNA damage in liver, lung and white blood cells nor into an increase in the % of MN in circulating reticulocytes. To the best of our knowledge, this was the first time that the genotoxic potential of AuNRs was investigated in zebrafish embryos. However, this organism has been employed to test other NMs, namely zinc oxide (ZnO) and TiO_2 NMs, which have been shown to cause significant DNA damage (Zhao, Wang et al. 2013, He, Aker et al. 2014). Other mechanisms might be responsible for the toxicity observed in zebrafish embryos exposed to CTAB-AuNRs such as oxidative stress. For instance, Wan et al. reported that CTAB-AuNRs with various aspect ratios were cytotoxic to tumor cells and non-malignant transformed cells by triggering mitochondrial damage and excessive ROS production (Wan, Wang et al. 2015).

6. Conclusion and Future Perspectives

This project aimed to investigate the toxicity of a commercial suspension of CTAB-AuNRs towards early life stages of zebrafish due to the potential environmental risk posed by NMs, whose demand is increasing exponentially in various areas such as biomedicine, electronics and catalysis.

The CTAB-AuNRs induced 50% of mortality ($LC_{50,96hpf}$) at a concentration of 110.2 µg/L. Furthermore, at sublethal concentrations it was found to elicit developmental abnormalities such as tail deformities, pericardial edema, decreased body length and development delays. Moreover, less than 1% of the initial CTAB-AuNRs present in the exposure media was internalized by zebrafish embryos before and after hatching. However, no DNA damage was induced by CTAB-AuNRs exposure. While mild malformations were observed, with a general all-or-nothing effect, the developmental delay observed coupled with the internalization of CTAB-AuNRs in the zebrafish tissue cannot be disregarded as structural or functional defects might emerge only at adult stages. Therefore, it would be interesting to evaluate the behavior (e.g. locomotor activity) of juvenile and adult stages previously exposed to CTAB-AuNRs, which might be indicative of ecological relevant effects such as feeding behavior disruption or increased susceptibility to predation that seriously compromise the fitness of the individual and the population.

The surfactant CTAB both adsorbed and freely dispersed in solution seems to account for the toxicity of the tested AuNRs. However, to identify the real extent of the CTAB contribution for the AuNRs hazard observed in zebrafish, it is essential to compare it with bare AuNRs. Nevertheless, the hypotheses raised here that AuNRs might in fact reduce the bioavailability of CTAB, thus retarding their toxicity, highlights the potential for AuNRs be employed for the selective and efficient removal of a variety of pollutants in water. In the other hand, it also fosters the necessity to improve the AuNRs production by replacing toxic compounds while maintaining the efficiency and yield of the syntheses, and keeping the desired properties of AuNRs, and/or by applying efficient purification techniques.

The internalization of AuNRs by zebrafish embryos should be further assessed by TEM analysis as it would allow to clarify if the Au content detected in zebrafish embryos at 48 hpf was due to the adsorption of AuNRs to the chorion or the effective accumulation inside zebrafish tissues.

Overall, CTAB-AuNRs caused significant lethal and sublethal effects at low concentrations, which might translate into fitness impairment at adult stages, highlighting the need to perform predictive risk assessment of these nanomaterials in

order to establish environmental safety values. Further research is needed to unravel the mechanism of action and the properties responsible for the AuNRs toxicity and thus support regulatory decisions that safeguard workers, consumers and the environment and ultimately, assist the development of safer NMs and manufacturing processes.

7. References

Alkilany, A. M. and C. J. Murphy (2010). "Toxicity and cellular uptake of gold nanoparticles: what we have learned so far?" Journal of nanoparticle research **12**(7): 2313-2333.

Alkilany, A. M., P. K. Nagaria, C. R. Hexel, T. J. Shaw, C. J. Murphy and M. D. Wyatt (2009). "Cellular uptake and cytotoxicity of gold nanorods: molecular origin of cytotoxicity and surface effects." small **5**(6): 701-708.

Alkilany, A. M., L. B. Thompson, S. P. Boulos, P. N. Sisco and C. J. Murphy (2012). "Gold nanorods: their potential for photothermal therapeutics and drug delivery, tempered by the complexity of their biological interactions." Advanced drug delivery reviews **64**(2): 190-199.

Amiard-Triquet, C., J. C. Amiard and C. Mouneyrac (2015). Aquatic Ecotoxicology: Advancing Tools for Dealing with Emerging Risks, Elsevier Science.

Amreddy, N., R. Muralidharan, A. Babu, M. Mehta, E. V. Johnson, Y. D. Zhao, A. Munshi and R. Ramesh (2015). "Tumor-targeted and pH-controlled delivery of doxorubicin using gold nanorods for lung cancer therapy." International journal of nanomedicine **10**: 6773.

Arora, S., J. M. Rajwade and K. M. Paknikar (2012). "Nanotoxicology and in vitro studies: the need of the hour." Toxicology and applied pharmacology **258**(2): 151-165.

Asharani, P., Y. Lianwu, Z. Gong and S. Valiyaveettil (2011). "Comparison of the toxicity of silver, gold and platinum nanoparticles in developing zebrafish embryos." Nanotoxicology **5**(1): 43-54.

Bailey, J., A. Oliveri and E. D. Levin (2013). "Zebrafish model systems for developmental neurobehavioral toxicology." Birth Defects Research Part C: Embryo Today: Reviews **99**(1): 14-23.

Balasubramanian, S. K., J. Jittiwat, J. Manikandan, C. N. Ong, L. E. Yu and W. Y. Ong (2010). "Biodistribution of gold nanoparticles and gene expression changes in the liver and spleen after intravenous administration in rats." Biomaterials **31**(8): 2034-2042.

Baptista, P. V., G. Doria, P. Quaresma, M. Cavadas, C. S. Neves, I. Gomes, P. Eaton, E. Pereira and R. Franco (2010). "Nanoparticles in molecular diagnostics." Progress in molecular biology and translational science **104**: 427-488.

Boccalon, M., S. Bidoggia, F. Romano, L. Gualandi, P. Franchi, M. Lucarini, P. Pengo and L. Pasquato (2015). "Gold nanoparticles as drug carriers: a contribution to the quest for basic principles for monolayer design." Journal of Materials Chemistry B **3**(3): 432-439.

Botha, T. L., K. Boodhia and V. Wepener (2016). "Adsorption, uptake and distribution of gold nanoparticles in Daphnia magna following long term exposure." Aquatic Toxicology **170**: 104-111.

Boxall, A. B., Q. Chaudhry, C. Sinclair, A. Jones, R. Aitken, B. Jefferson and C. Watts (2007). "Current and future predicted environmental exposure to engineered nanoparticles." Central Science Laboratory, Department of the Environment and Rural Affairs, London, UK **89**.

Bozich, J. S., S. E. Lohse, M. D. Torelli, C. J. Murphy, R. J. Hamers and R. D. Klaper (2014). "Surface chemistry, charge and ligand type impact the toxicity of gold nanoparticles to Daphnia magna." Environmental Science: Nano **1**(3): 260-270.

Braunbeck, T., B. Kais, E. Lammer, J. Otte, K. Schneider, D. Stengel and R. Strecker (2015). "The fish embryo test (FET): origin, applications, and future." Environmental Science and Pollution Research **22**(21): 16247-16261.

Brenner, S. A., N. M. Neu-Baker, C. Caglayan and I. G. Zurbenko (2015). "Occupational exposure to airborne nanomaterials: an assessment of worker exposure to aerosolized metal oxide nanoparticles in semiconductor wastewater treatment." Journal of occupational and environmental hygiene **12**(7): 469-481.

Browning, L. M., T. Huang and X.-H. N. Xu (2013). "Real-time in vivo imaging of size-dependent transport and toxicity of gold nanoparticles in zebrafish embryos using single nanoparticle plasmonic spectroscopy." Interface focus **3**(3): 20120098.

Browning, L. M., K. J. Lee, T. Huang, P. D. Nallathamby, J. E. Lowman and X.-H. N. Xu (2009). "Random walk of single gold nanoparticles in zebrafish embryos leading to stochastic toxic effects on embryonic developments." Nanoscale **1**(1): 138-152.

Burrows, N. D., A. M. Vartanian, N. S. Abadeer, E. M. Grzincic, L. M. Jacob, W. Lin, J. Li, J. M. Dennison, J. G. Hinman and C. J. Murphy (2016). "Anisotropic nanoparticles and anisotropic surface chemistry." The journal of physical chemistry letters **7**(4): 632-641.

Chen, Y.-S., Y.-C. Hung, I. Liau and G. S. Huang (2009). "Assessment of the in vivo toxicity of gold nanoparticles." Nanoscale research letters **4**(8): 858-864.

Cho, W.-S., M. Cho, J. Jeong, M. Choi, H.-Y. Cho, B. S. Han, S. H. Kim, H. O. Kim, Y. T. Lim and B. H. Chung (2009). "Acute toxicity and pharmacokinetics of 13 nm-sized PEG-coated gold nanoparticles." Toxicology and applied pharmacology **236**(1): 16-24.

Chu, M., Q. Wu, H. Yang, R. Yuan, S. Hou, Y. Yang, Y. Zou, S. Xu, K. Xu and A. Ji (2010). "Transfer of quantum dots from pregnant mice to pups across the placental barrier." Small **6**(5): 670-678.

Commission, E. (2011). COMMISSION RECOMMENDATION of 18 October 2011 on the definition of nanomaterial. Official Journal of the European Union

Di Bucchianico, S., M. R. Fabbrizi, S. Cirillo, C. Uboldi, D. Gilliland, E. Valsami-Jones and L. Migliore (2014). "Aneuploidogenic effects and DNA oxidation induced in vitro by differently sized gold nanoparticles." International journal of nanomedicine **9**: 2191.

Downs, T. R., M. E. Crosby, T. Hu, S. Kumar, A. Sullivan, K. Sarlo, B. Reeder, M. Lynch, M. Wagner and T. Mills (2012). "Silica nanoparticles administered at the maximum tolerated dose induce genotoxic effects through an inflammatory reaction while gold nanoparticles do not." Mutation Research/Genetic Toxicology and Environmental Mutagenesis **745**(1): 38-50.

Dusinska, M., Z. Magdolenova and L. M. Fjellsbø (2013). Toxicological aspects for nanomaterial in humans. Nanotechnology for Nucleic Acid Delivery, Springer**:** 1-12.

Dutta, S. (2015). "Human teratogens and their effects: a critical evaluation." International Journal of Information Research and Review.

Elci, S. G., Y. Jiang, B. Yan, S. T. Kim, K. Saha, D. F. Moyano, G. Yesilbag Tonga, L. C. Jackson, V. M. Rotello and R. W. Vachet (2016). "Surface Charge Controls the Sub-Organ Biodistributions of Gold Nanoparticles." ACS nano.

Embry, M. R., S. E. Belanger, T. A. Braunbeck, M. Galay-Burgos, M. Halder, D. E. Hinton, M. A. Léonard, A. Lillicrap, T. Norberg-King and G. Whale (2010). "The fish embryo toxicity test as an animal alternative method in hazard and risk assessment and scientific research." Aquatic Toxicology **97**(2): 79-87.

Fadeel, B. and A. Pietroiusti (2012). Adverse Effects of Engineered Nanomaterials: Exposure, Toxicology, and Impact on Human Health, Elsevier Science.

Fang, T., L. Yu, W. Zhang and S. Bao (2015). "Effects of humic acid and ionic strength on TiO2 nanoparticles sublethal toxicity to zebrafish." Ecotoxicology **24**(10): 2054-2066.

Ferreira, P., E. Fonte, M. E. Soares, F. Carvalho and L. Guilhermino (2016). "Effects of multi-stressors on juveniles of the marine fish Pomatoschistus microps: Gold nanoparticles, microplastics and temperature." Aquatic Toxicology **170**: 89-103.

Ferry, J. L., P. Craig, C. Hexel, P. Sisco, R. Frey, P. L. Pennington, M. H. Fulton, I. G. Scott, A. W. Decho and S. Kashiwada (2009). "Transfer of gold nanoparticles from the water column to the estuarine food web." Nature Nanotechnology **4**(7): 441-444.

Foss Jr, C. A., G. L. Hornyak, J. A. Stockert and C. R. Martin (1992). "Optical properties of composite membranes containing arrays of nanoscopic gold cylinders." The Journal of Physical Chemistry **96**(19): 7497-7499.

Fraga, S., A. Brandao, M. E. Soares, T. Morais, J. A. Duarte, L. Pereira, L. Soares, C. Neves, E. Pereira, L. Bastos Mde and H. Carmo (2014). "Short- and long-term distribution and toxicity of gold nanoparticles in the rat after a single-dose intravenous administration." Nanomedicine **10**(8): 1757-1766.

Fraga, S., H. Faria, M. E. Soares, J. A. Duarte, L. Soares, E. Pereira, C. Costa-Pereira, J. P. Teixeira, M. Lourdes Bastos and H. Carmo (2013). "Influence of the surface coating on the cytotoxicity, genotoxicity and uptake of gold nanoparticles in human HepG2 cells." Journal of Applied Toxicology **33**(10): 1111-1119.

Frens, G. (1973). "Controlled nucleation for the regulation of the particle size in monodisperse gold suspensions." Nature **241**(105): 20-22.

Galindo, T. (2014). Nanomaterials: Assessing the influence of several factors on their ecotoxicity to biota Philosophiæ Doctor (PhD), Aveiro University.

Galindo, T., R. Pereira, A. Freitas, T. Santos-Rocha, M. Rasteiro, F. Antunes, D. Rodrigues, A. Soares, F. Gonçalves and A. Duarte (2013). "Toxicity of organic and inorganic nanoparticles to four species of white-rot fungi." Science of the total environment **458**: 290-297.

García-Cambero, J. P., M. N. García, G. D. López, A. L. Herranz, L. Cuevas, E. Pérez-Pastrana, J. S. Cuadal, M. R. Castelltort and A. C. Calvo (2013). "Converging hazard assessment of gold nanoparticles to aquatic organisms." Chemosphere **93**(6): 1194-1200.

Ghosh, P., G. Han, M. De, C. K. Kim and V. M. Rotello (2008). "Gold nanoparticles in delivery applications." Advanced drug delivery reviews **60**(11): 1307-1315.

Girgis, E., W. Khalil, A. Emam, M. Mohamed and K. V. Rao (2012). "Nanotoxicity of gold and gold–cobalt nanoalloy." Chemical research in toxicology **25**(5): 1086-1098.

Golbamaki, N., B. Rasulev, A. Cassano, R. L. M. Robinson, E. Benfenati, J. Leszczynski and M. T. Cronin (2015). "Genotoxicity of metal oxide nanomaterials: review of recent data and discussion of possible mechanisms." Nanoscale **7**(6): 2154-2198.

Gottschalk, F., T. Sun and B. Nowack (2013). "Environmental concentrations of engineered nanomaterials: review of modeling and analytical studies." Environmental Pollution **181**: 287-300.

Grafmüller, S., P. Manser, H. F. Krug, P. Wick and U. von Mandach (2013). "Determination of the transport rate of xenobiotics and nanomaterials across the placenta using the ex vivo human placental perfusion model." Journal of visualized experiments: JoVE(76).

Grzelczak, M., J. Pérez-Juste, P. Mulvaney and L. M. Liz-Marzán (2008). "Shape control in gold nanoparticle synthesis." Chemical Society Reviews **37**(9): 1783-1791.

Gui, C. and D.-x. Cui (2012). "Functionalized gold nanorods for tumor imaging and targeted therapy." Cancer Biology & Medicine **9**(4): 221-233.

Han, S. G., J. S. Lee, K. Ahn, Y. S. Kim, J. K. Kim, J. H. Lee, J. H. Shin, K. S. Jeon, W. S. Cho, N. W. Song, M. Gulumian, B. S. Shin and I. J. Yu (2015). "Size-dependent clearance of gold nanoparticles from

lungs of Sprague–Dawley rats after short-term inhalation exposure." Archives of Toxicology **89**(7): 1083-1094.

Hansen, J. M. and C. Harris (2013). "Redox control of teratogenesis." Reproductive Toxicology **35**: 165-179.

Hashimoto, M., K. Kawai, H. Kawakami and S. Imazato (2016). "Matrix metalloproteases inhibition and biocompatibility of gold and platinum nanoparticles." Journal of Biomedical Materials Research Part A **104**(1): 207-215.

He, J.-H., J.-M. Gao, C.-J. Huang and C.-Q. Li (2014). "Zebrafish models for assessing developmental and reproductive toxicity." Neurotoxicology and teratology **42**: 35-42.

He, X., W. G. Aker and H.-M. Hwang (2014). "An in vivo study on the photo-enhanced toxicities of S-doped TiO2 nanoparticles to zebrafish embryos (Danio rerio) in terms of malformation, mortality, rheotaxis dysfunction, and DNA damage." Nanotoxicology **8**(sup1): 185-195.

Hinman, J. G., A. Stork, J. A. Varnell, A. Gewirth and C. Murphy (2016). "Seed Mediated Growth of Gold Nanorods: Towards Nanorod Matryoshkas." Faraday Discussions.

Howes, P. D., S. Rana and M. M. Stevens (2014). "Plasmonic nanomaterials for biodiagnostics." Chemical Society Reviews **43**(11): 3835-3853.

Huang, S., P. J. Chueh, Y.-W. Lin, T.-S. Shih and S.-M. Chuang (2009). "Disturbed mitotic progression and genome segregation are involved in cell transformation mediated by nano-TiO2 long-term exposure." Toxicology and applied pharmacology **241**(2): 182-194.

Huang, X. and M. A. El-Sayed (2010). "Gold nanoparticles: optical properties and implementations in cancer diagnosis and photothermal therapy." Journal of Advanced Research **1**(1): 13-28.

Initiative, U. S. N. N. (2016). "Environmental, Health, and Safety Issues." Retrieved September 2016, from http://www.nano.gov/you/environmental-health-safety.

Insights, G. M. (2016). "Gold Nanoparticles Market Size By Application (Electronics, Medical & Dentistry,Catalysis), Industry Analysis Report, Regional Outlook, Application Potential, Price Trend, Competitive Market Share & Forecast, 2015 – 2022."

Jana, N. R., L. Gearheart and C. J. Murphy (2001). "Wet chemical synthesis of high aspect ratio cylindrical gold nanorods." The Journal of Physical Chemistry B **105**(19): 4065-4067.

Janát-Amsbury, M., A. Ray, C. Peterson and H. Ghandehari (2011). "Geometry and surface characteristics of gold nanoparticles influence their biodistribution and uptake by macrophages." European Journal of Pharmaceutics and Biopharmaceutics **77**(3): 417-423.

Kaegi, R., B. Sinnet, S. Zuleeg, H. Hagendorfer, E. Mueller, R. Vonbank, M. Boller and M. Burkhardt (2010). "Release of silver nanoparticles from outdoor facades." Environmental pollution **158**(9): 2900-2905.

Kaegi, R., A. Ulrich, B. Sinnet, R. Vonbank, A. Wichser, S. Zuleeg, H. Simmler, S. Brunner, H. Vonmont and M. Burkhardt (2008). "Synthetic TiO 2 nanoparticle emission from exterior facades into the aquatic environment." Environmental pollution **156**(2): 233-239.

Khan, M. S., G. D. Vishakante and H. Siddaramaiah (2013). "Gold nanoparticles: a paradigm shift in biomedical applications." Advances in colloid and interface science **199**: 44-58.

Kim, F., J. H. Song and P. Yang (2002). "Photochemical synthesis of gold nanorods." Journal of the American Chemical Society **124**(48): 14316-14317.

Kim, K.-T., T. Zaikova, J. E. Hutchison and R. L. Tanguay (2013). "Gold nanoparticles disrupt zebrafish eye development and pigmentation." toxicological sciences **133**(2): 275-288.

Kimmel, C. B., W. W. Ballard, S. R. Kimmel, B. Ullmann and T. F. Schilling (1995). "Stages of embryonic development of the zebrafish." Developmental dynamics **203**(3): 253-310.

Kosmehl, T., A. V. Hallare, G. Reifferscheid, W. Manz, T. Braunbeck and H. Hollert (2006). "A novel contact assay for testing genotoxicity of chemicals and whole sediments in zebrafish embryos." Environmental toxicology and chemistry **25**(8): 2097-2106.

Kumar, A., X. Zhang and X.-J. Liang (2013). "Gold nanoparticles: emerging paradigm for targeted drug delivery system." Biotechnology advances **31**(5): 593-606.

Lee, W.-M., S.-J. Yoon, Y.-J. Shin and Y.-J. An (2015). "Trophic transfer of gold nanoparticles from Euglena gracilis or Chlamydomonas reinhardtii to Daphnia magna." Environmental Pollution **201**: 10-16.

Leifert, A., Y. Pan-Bartnek, U. Simon and W. Jahnen-Dechent (2013). "Molecularly stabilised ultrasmall gold nanoparticles: synthesis, characterization and bioactivity." Nanoscale **5**(14): 6224-6242.

Lewinski, N., V. Colvin and R. Drezek (2008). "Cytotoxicity of nanoparticles." small **4**(1): 26-49.

Li, J. J., S.-L. Lo, C.-T. Ng, R. L. Gurung, D. Hartono, M. P. Hande, C.-N. Ong, B.-H. Bay and L.-Y. L. Yung (2011). "Genomic instability of gold nanoparticle treated human lung fibroblast cells." Biomaterials **32**(23): 5515-5523.

MacRae, C. A. and R. T. Peterson (2015). "Zebrafish as tools for drug discovery." Nature Reviews Drug Discovery **14**(10): 721-731.

Magdolenova, Z., A. Collins, A. Kumar, A. Dhawan, V. Stone and M. Dusinska (2014). "Mechanisms of genotoxicity. A review of in vitro and in vivo studies with engineered nanoparticles." Nanotoxicology **8**(3): 233-278.

Mahapatra, I., T. Y. Sun, J. R. Clark, P. J. Dobson, K. Hungerbuehler, R. Owen, B. Nowack and J. Lead (2015). "Probabilistic modelling of prospective environmental concentrations of gold nanoparticles from medical applications as a basis for risk assessment." Journal of nanobiotechnology **13**(1): 1.

Mahmoudi, M., I. Lynch, M. R. Ejtehadi, M. P. Monopoli, F. B. Bombelli and S. Laurent (2011). "Protein− nanoparticle interactions: opportunities and challenges." Chemical reviews **111**(9): 5610-5637.

Manheller, M. (2012). Optical and Electrical Addressing in Molecule-based Logic Circuits, Forschungszentrum Jülich, Zentralbibliothek.

Maynard, A. D., P. A. Baron, M. Foley, A. A. Shvedova, E. R. Kisin and V. Castranova (2004). "Exposure to carbon nanotube material: aerosol release during the handling of unrefined single-walled carbon nanotube material." Journal of Toxicology and Environmental Health, Part A **67**(1): 87-107.

McWilliams, A. (2014). Nanotechnology: A Realistic Market Assessment, BCC Research.

Monopoli, M. P., C. Åberg, A. Salvati and K. A. Dawson (2012). "Biomolecular coronas provide the biological identity of nanosized materials." Nature nanotechnology **7**(12): 779-786.

Morais, T., M. E. Soares, J. A. Duarte, L. Soares, S. Maia, P. Gomes, E. Pereira, S. Fraga, H. Carmo and L. Bastos Mde (2012). "Effect of surface coating on the biodistribution profile of gold nanoparticles in the rat." Eur J Pharm Biopharm **80**(1): 185-193.

Murphy, C. J., L. B. Thompson, D. J. Chernak, J. A. Yang, S. T. Sivapalan, S. P. Boulos, J. Huang, A. M. Alkilany and P. N. Sisco (2011). "Gold nanorod crystal growth: from seed-mediated synthesis to nanoscale sculpting." Current Opinion in Colloid & Interface Science **16**(2): 128-134.

Myllynen, P. K., M. J. Loughran, C. V. Howard, R. Sormunen, A. A. Walsh and K. H. Vähäkangas (2008). "Kinetics of gold nanoparticles in the human placenta." Reproductive toxicology **26**(2): 130-137.

Nanotechnologies, T. P. O. E. (2013). Consumer Products Inventory.

Nel, A. E., W. J. Parak, W. C. Chan, T. Xia, M. C. Hersam, C. J. Brinker, J. I. Zink, K. E. Pinkerton, D. R. Baer and P. S. Weiss (2015). "Where are we heading in nanotechnology environmental health and safety and materials characterization?" ACS nano **9**(6): 5627-5630.

North, T. E., W. Goessling, C. R. Walkley, C. Lengerke, K. R. Kopani, A. M. Lord, G. J. Weber, T. V. Bowman, I.-H. Jang and T. Grosser (2007). "Prostaglandin E2 regulates vertebrate haematopoietic stem cell homeostasis." Nature **447**(7147): 1007-1011.

Oberdörster, G., E. Oberdörster and J. Oberdörster (2005). "Nanotoxicology: an emerging discipline evolving from studies of ultrafine particles." Environmental health perspectives: 823-839.

OCDE (2008). GUIDANCE DOCUMENT ON MAMMALIAN REPRODUCTIVE TOXICITY TESTING AND ASSESSMENT Organisation For Economic Co-Operation And Development **43**.

OECD (1992). Test No. 203: Fish, Acute Toxicity Test, OECD Publishing.

OECD (2013). Test No. 236: Fish Embryo Acute Toxicity (FET) Test, OECD Publishing.

Olive, P. L. and J. P. Banath (2006). "The comet assay: a method to measure DNA damage in individual cells." Nat. Protocols **1**(1): 23-29.

Pan, J.-F., P.-E. Buffet, L. Poirier, C. Amiard-Triquet, D. Gilliland, Y. Joubert, P. Pilet, M. Guibbolini, C. R. de Faverney and M. Roméo (2012). "Size dependent bioaccumulation and ecotoxicity of gold nanoparticles in an endobenthic invertebrate: the Tellinid clam Scrobicularia plana." Environmental pollution **168**: 37-43.

Pan, Y., A. Leifert, M. Graf, F. Schiefer, S. Thoröe-Boveleth, J. Broda, M. C. Halloran, H. Hollert, D. Laaf and U. Simon (2013). "High-Sensitivity Real-Time Analysis of Nanoparticle Toxicity in Green Fluorescent Protein-Expressing Zebrafish." Small **9**(6): 863-869.

Peters, R. H. (1986). The ecological implications of body size, Cambridge University Press.

Qian, H., L. A. Pretzer, J. C. Velazquez, Z. Zhao and M. S. Wong (2013). "Gold nanoparticles for cleaning contaminated water." Journal of Chemical Technology and Biotechnology **88**(5): 735-741.

Roos, W. P., A. D. Thomas and B. Kaina (2015). "DNA damage and the balance between survival and death in cancer biology." Nature Reviews Cancer.

Rosenthal, N. and R. P. Harvey (2010). Heart Development and Regeneration, Elsevier Science.

Saha, K., S. S. Agasti, C. Kim, X. Li and V. M. Rotello (2012). "Gold nanoparticles in chemical and biological sensing." Chemical reviews **112**(5): 2739-2779.

Sandbacka, M., I. Christianson and B. Isomaa (2000). "The acute toxicity of surfactants on fish cells, Daphnia magna and fish—A comparative study." Toxicology in Vitro **14**(1): 61-68.

Scarabelli, L., A. Sánchez-Iglesias, J. Pérez-Juste and L. M. Liz-Marzán (2015). "A “Tips and Tricks” Practical Guide to the Synthesis of Gold Nanorods." The journal of physical chemistry letters **6**(21): 4270-4279.

Scholz, S., S. Fischer, U. Gündel, E. Küster, T. Luckenbach and D. Voelker (2008). "The zebrafish embryo model in environmental risk assessment—applications beyond acute toxicity testing." Environmental Science and Pollution Research **15**(5): 394-404.

Schulz, M., L. Ma-Hock, S. Brill, V. Strauss, S. Treumann, S. Gröters, B. van Ravenzwaay and R. Landsiedel (2012). "Investigation on the genotoxicity of different sizes of gold nanoparticles administered

to the lungs of rats." Mutation Research/Genetic Toxicology and Environmental Mutagenesis **745**(1): 51-57.

Semmler-Behnke, M., J. Lipka, A. Wenk, S. Hirn, M. Schäffler, F. Tian, G. Schmid, G. Oberdörster and W. G. Kreyling (2014). "Size dependent translocation and fetal accumulation of gold nanoparticles from maternal blood in the rat." Particle and fibre toxicology **11**(1): 1-12.

Semmler-Behnke, M., W. G. Kreyling, J. Lipka, S. Fertsch, A. Wenk, S. Takenaka, G. Schmid and W. Brandau (2008). "Biodistribution of 1.4-and 18-nm Gold Particles in Rats." Small **4**(12): 2108-2111.

Senut, M. C., Y. Zhang, F. Liu, A. Sen, D. M. Ruden and G. Mao (2015). "Size-Dependent Toxicity of Gold Nanoparticles on Human Embryonic Stem Cells and Their Neural Derivatives." Small.

Singh, N. P., M. T. McCoy, R. R. Tice and E. L. Schneider (1988). "A simple technique for quantitation of low levels of DNA damage in individual cells." Experimental cell research **175**(1): 184-191.

Singh, S., V. D'Britto, A. Prabhune, C. Ramana, A. Dhawan and B. Prasad (2010). "Cytotoxic and genotoxic assessment of glycolipid-reduced and-capped gold and silver nanoparticles." New Journal of Chemistry **34**(2): 294-301.

Söderstjerna, E., F. Johansson, B. Klefbohm and U. Englund Johansson (2013). "Gold-and silver nanoparticles affect the growth characteristics of human embryonic neural precursor cells." PloS one **8**(3).

Stegeman, J. J., J. V. Goldstone and M. E. Hahn (2010). "10-Perspectives on zebrafish as a model in environmental toxicology." Fish Physiology **29**: 367-439.

Sun, T. Y., F. Gottschalk, K. Hungerbühler and B. Nowack (2014). "Comprehensive probabilistic modelling of environmental emissions of engineered nanomaterials." Environmental Pollution **185**: 69-76.

Taylor, U., W. Garrels, A. Barchanski, S. Peterson, L. Sajti, A. Lucas-Hahn, L. Gamrad, U. Baulain, S. Klein and W. A. Kues (2014). "Injection of ligand-free gold and silver nanoparticles into murine embryos does not impact pre-implantation development." Beilstein journal of nanotechnology **5**(1): 677-688.

Teles, M., C. Fierro-Castro, P. Na-Phatthalung, A. Tvarijonaviciute, T. Trindade, A. Soares, L. Tort and M. Oliveira (2016). "Assessment of gold nanoparticle effects in a marine teleost (Sparus aurata) using molecular and biochemical biomarkers." Aquatic Toxicology **177**: 125-135.

Tiwari, J. N., R. N. Tiwari and K. S. Kim (2012). "Zero-dimensional, one-dimensional, two-dimensional and three-dimensional nanostructured materials for advanced electrochemical energy devices." Progress in Materials Science **57**(4): 724-803.

Truong, L., K. S. Saili, J. M. Miller, J. E. Hutchison and R. L. Tanguay (2012). "Persistent adult zebrafish behavioral deficits results from acute embryonic exposure to gold nanoparticles." Comparative Biochemistry and Physiology Part C: Toxicology & Pharmacology **155**(2): 269-274.

Truong, L., S. C. Tilton, T. Zaikova, E. Richman, K. M. Waters, J. E. Hutchison and R. L. Tanguay (2013). "Surface functionalities of gold nanoparticles impact embryonic gene expression responses." Nanotoxicology **7**(2): 192-201.

Truong, L., T. Zaikova, E. K. Richman, J. E. Hutchison and R. L. Tanguay (2012). "Media ionic strength impacts embryonic responses to engineered nanoparticle exposure." Nanotoxicology **6**(7): 691-699.

Turkevich, J., P. C. Stevenson and J. Hillier (1951). "A study of the nucleation and growth processes in the synthesis of colloidal gold." Discussions of the Faraday Society **11**: 55-75.

Uusi-Heikkilä, S., A. Kuparinen, C. Wolter, T. Meinelt and R. Arlinghaus (2012). "Paternal body size affects reproductive success in laboratory-held zebrafish (Danio rerio)." Environmental biology of fishes **93**(4): 461-474.

Völker, C., C. Boedicker, J. Daubenthaler, M. Oetken and J. Oehlmann (2013). "Comparative toxicity assessment of nanosilver on three Daphnia species in acute, chronic and multi-generation experiments." PloS one **8**(10): e75026.

Wan, J., J.-H. Wang, T. Liu, Z. Xie, X.-F. Yu and W. Li (2015). "Surface chemistry but not aspect ratio mediates the biological toxicity of gold nanorods in vitro and in vivo." Scientific reports **5**.

Wan, R., Y. Mo, L. Feng, S. Chien, D. J. Tollerud and Q. Zhang (2012). "DNA Damage Caused by Metal Nanoparticles: Involvement of Oxidative Stress and Activation of ATM†." Chemical research in toxicology **25**(7): 1402-1411.

Wang, Z., D. Xie, H. Liu, Z. Bao and Y. Wang (2016). "Toxicity assessment of precise engineered gold nanoparticles with different shapes in zebrafish embryos." RSC Advances **6**(39): 33009-33013.

Wang, Z., L. Zhang, J. Zhao and B. Xing (2016). "Environmental processes and toxicity of metallic nanoparticles in aquatic systems as affected by natural organic matter." Environmental Science: Nano **3**(2): 240-255.

Warheit, D. B. and C. M. Sayes (2015). "Routes of Exposure to Nanoparticles: Hazard Tests Related to Portal Entries." Nanoengineering: Global Approaches to Health and Safety Issues: 41.

Xia, K., L. Zhang, Y. Huang and Z. Lu (2015). "Preparation of gold nanorods and their applications in photothermal therapy." Journal of nanoscience and nanotechnology **15**(1): 63-73.

Yang, H., C. Sun, Z. Fan, X. Tian, L. Yan, L. Du, Y. Liu, C. Chen, X.-j. Liang and G. J. Anderson (2012). "Effects of gestational age and surface modification on materno-fetal transfer of nanoparticles in murine pregnancy." Scientific reports **2**.

Yang, L., N. Y. Ho, R. Alshut, J. Legradi, C. Weiss, M. Reischl, R. Mikut, U. Liebel, F. Müller and U. Strähle (2009). "Zebrafish embryos as models for embryotoxic and teratological effects of chemicals." Reproductive Toxicology **28**(2): 245-253.

Yu, Y.-Y., S.-S. Chang, C.-L. Lee and C. C. Wang (1997). "Gold nanorods: electrochemical synthesis and optical properties." The Journal of Physical Chemistry B **101**(34): 6661-6664.

Zhang, X.-D., H.-Y. Wu, D. Wu, Y.-Y. Wang, J.-H. Chang, Z.-B. Zhai, A.-M. Meng, P.-X. Liu, L.-A. Zhang and F.-Y. Fan (2010). "Toxicologic effects of gold nanoparticles in vivo by different administration routes." International Journal of Nanomedicine **5**: 771-781.

Zhao, X., S. Wang, Y. Wu, H. You and L. Lv (2013). "Acute ZnO nanoparticles exposure induces developmental toxicity, oxidative stress and DNA damage in embryo-larval zebrafish." Aquatic Toxicology **136–137**: 49-59.

Zhou, W., X. Gao, D. Liu and X. Chen (2015). "Gold nanoparticles for in vitro diagnostics." Chemical reviews **115**(19): 10575-10636.

Zhu, X., J. Wang, X. Zhang, Y. Chang and Y. Chen (2010). "Trophic transfer of TiO(2) nanoparticles from Daphnia to zebrafish in a simplified freshwater food chain." Chemosphere **79**(9): 928-933.